VARIABILITY IN SULFUR ISOTOPE RECORDS OF PHANEROZOIC SEAWATER SULFATE

Theodore M. Present[1], Jess F. Adkins[1], and Woodward W. Fischer[1]

[1]California Institute of Technology, Pasadena, California, USA

Corresponding author: Theodore M. Present (ted@caltech.edu)

Key Points

- 6710 measurements of $\delta^{34}S$ of sulfate in Phanerozoic sedimentary rocks were compiled and systematically updated to a consistent time scale
- Records derived from evaporites, barite, and carbonate-associated sulfate are similar, but also contain dramatic short-term discrepancies
- Variation created by diagenetic and depositional processes increases with age in all records, obscuring temporal trends in marine sulfate

Plain Language Summary

Sedimentary rocks deposited in ancient oceans preserve a record of seawater composition. We compare the sulfur isotopic composition of three sedimentary materials that contain sulfate—a major ion in seawater important for carbon and oxygen cycling. Evaporite salts, the mineral barite, and trace sulfate in limestone each have the same first-order trends over the last 541 million years, but also display substantial shorter order discrepancies that reflect how the materials capture and store paleooceanographic information. These discrepancies partially obscure understanding of the relationship between life, ocean chemistry, and climate.

Keywords

Phanerozoic seawater composition; marine sulfate proxies; carbonate-associated sulfate; evaporites; barite; sulfur isotope ratios; kriging

Abstract

The $\delta^{34}S$ of seawater sulfate reflects processes operating at the nexus of sulfur, carbon, and dioxygen cycles. However, knowledge of past seawater sulfate $\delta^{34}S$ values must be derived from proxy materials that are impacted differently by depositional and post-depositional processes. We produced new timeseries estimates for the $\delta^{34}S$ value of seawater sulfate by combining 6710 published data from three sedimentary archives—marine barite, evaporites, and carbonate-associated sulfate—with updated age constraints on the deposits. Robust features in the records capture temporal trends in the $\delta^{34}S$ value of seawater and its interplay with other Phanerozoic geochemical and stratigraphic trends. However, high-frequency discordances demonstrate that each record is differentially prone to depositional biases and diagenetic overprints. The amount of noise, quantified from the variograms of each record, increases with age for all $\delta^{34}S$ proxies, indicating that post-depositional processes obscure detailed knowledge of seawater sulfate's $\delta^{34}S$ value deeper in time.

1 Introduction

Seawater sulfate acts as a major oxidant of organic carbon, controlling the cadence of its burial in sediments and connecting the carbon and sulfur cycles (Bowles et al., 2014; Jørgensen, 1982). Microbial sulfate reduction (MSR), reoxidation of sulfide, and the burial and oxidation of pyrite govern sedimentary inorganic carbon and alkalinity fluxes (Ben-Yaakov, 1973; Froelich et al., 1979). Pyrite in sedimentary rocks may be exposed and oxidized during uplift, erosion, and weathering, impacting the dioxygen and carbon dioxide budgets on tectonic timescales (Burke et al., 2018; Kump & Garrels, 1986; M. A. Torres et al., 2014). Over Phanerozoic time (the past 541 Myr), the burial of sulfide and disulfide minerals must eventually balance the acid produced and dioxygen consumed during terrestrial pyrite weathering. Therefore, tracking ancient sulfate fluxes related to these processes illuminates when, how, and where the Earth system achieves this balance, and what happens during intervals of unsteadiness.

Thode et al. (1953) first recognized that a record of ancient marine sulfur isotopic compositions ($\delta^{34}S$) could inform changes to Earth's biogeochemical cycles, and Ault and Kulp (1959) applied mass balance assumptions in an early effort to quantify important sulfur fluxes. Isotope fractionations during MSR preferentially enrich the residual sulfate in ^{34}S (Harrison & Thode, 1958). Thus, when more sulfate is reduced and fixed into pyrite, removing more light sulfur isotopes from the oceans, the remaining sulfate in seawater becomes enriched in the heavy, rare isotopes. Holland (1973) first attempted to calculate changes in dioxygen fluxes from $\delta^{34}S$ data. Holser (1977) further recognized that rapid changes in the $\delta^{34}S$ value of seawater coincide with intervals of biotic crises and dramatic reorganizations of Earth's climate and biosphere. The subsequent forty years have seen many efforts to derive an accurate and precise record of how the $\delta^{34}S$ value of seawater sulfate has changed over Earth history.

Three sedimentary materials constitute proxy archives of $\delta^{34}S$ values of Phanerozoic seawater sulfate: (1) marine evaporites, which include sulfate salts precipitated from evaporated seawater in marginal marine basins; (2) marine barite, which forms from a suite of biogeochemical processes associated with sinking particles and early diagenesis in pelagic waters; and (3) carbonate-associated sulfate (CAS), which is minor sulfate incorporated into the crystal lattice of biogenic and abiogenic calcite, aragonite, and dolomite phases that accumulate in sedimentary rocks. Important reviews (Bottrell & Newton, 2006; Claypool et al., 1980; Holser et al., 1989; Strauss, 1997; Veizer et al., 1980) on the evolution of the Phanerozoic sulfur cycle have assumed that these proxies accurately preserve the isotopic composition of ancient seawater sulfate.

We produced a new timeseries to estimate the Phanerozoic history of the $\delta^{34}S$ value of seawater sulfate by synthesizing published geochemical data with updated geochronology and stratigraphic correlations. From this record we quantified the differences exhibited between the archives, which we attribute to mechanics of how sulfate is incorporated into and preserved in sedimentary rocks.

2 Synthesis of Phanerozoic seawater sulfate $\delta^{34}S$ proxy data

We compiled 6710 measurements from 108 references that analyzed $\delta^{34}S$ values in Phanerozoic marine evaporites, bulk rock CAS, biogenic CAS, or marine barite. Some previous evaporite $\delta^{34}S$ compilations included data from salt diapirs, secondary veins in non-sedimentary rocks, aqueous brines that had dissolved nearby evaporite-bearing formations, or brackish or non-marine depositional environments; these data were excluded from this compilation. The bulk rock CAS record contains data from sedimentary carbonate phases, although the extraction procedure employed varies between studies. The biogenic CAS record includes CAS data from brachiopods, belemnites, bivalves, and foraminifera, as well as sulfate in apatite from conodonts. Although preservation of biogenic and bulk-rock CAS was addressed in each reference, all data were included in the current compilation. Sulfur isotope data from authigenic phosphorites were not included.

Each $\delta^{34}S$ value was assigned an age using the International Commission on Stratigraphy 2016/04 time scale (Cohen et al., 2013; updated) (Figure 1). For data from studies that included radiometric ages, the radiometric age model was maintained. For studies that included stage-level assignments of the lithostratigraphy, ages were assigned by linearly interpolating on stratigraphic thickness unless the reference included independent estimates of sedimentation rate. For studies that assigned ages but did not include stratigraphic data, ages were updated by linearly interpolating between the assigned ages of stage boundaries in each time scale. The $\delta^{34}S$ data and stratigraphic height or age assignment was extracted graphically from figures in references that did not tabulate data. Many evaporite deposits have substantially improved stratigraphic and age assignments since publication of their sulfur isotope data. The ages of evaporite-bearing formations have been updated using the most recent tectono-stratigraphy and/or economic exploration literature. The Supporting

Information enumerates the $\delta^{34}S$ data, assigned age, data type, data source, and method and literature used for each age assignment.

Each proxy material has different, irregularly spaced temporal distributions (Figure 1a). To estimate Phanerozoic $\delta^{34}S$ trends, each proxy record was interpolated at 500 kyr resolution (Figure 1b). Kriging—a geostatistical approach using autocorrelation to quantify stochastic components in spatiotemporal data—was used to weight data for interpolation and estimate confidence intervals (Gebbers, 2010). Kriging weights the data between two endmembers of linearly detrended variance. At the maximum is the variance of all points in that geologic interval, and at the minimum is the unresolved chatter between data closely spaced in time. Variance increases from low values at the shortest separation distances to the population variance with the assumption that spatiotemporal processes are most correlated over short intervals. The kriged uncertainty on the interpolations reflects this increase in variance, such that interpolated values further from data have larger uncertainties up to the population variance according to the observed range of autocorrelation. Kriging was done on each geologic material, partitioned by era, by modelling variograms, which are functions describing how the variance per point (semivariance) of pairs of linearly detrended data varies with their average separation distance in time (Supporting Information). A circular variogram model, which represents the expected correlation between data arranged according to a Poisson distribution within two overlapping circles (Webster & Oliver, 2007), was used to create kriging estimates of the interpolated $\delta^{34}S$ values and variance.

Figure 1 ***[next page]*****.** Records of Phanerozoic seawater sulfate $\delta^{34}S$ generated from proxy materials. **(a)** The number of $\delta^{34}S$ analyses of each proxy per Myr, in 5 Myr bins, illustrates the temporal bias in the sampling of each material through Phanerozoic time. **(b)** Interpolated proxy records of the $\delta^{34}S$ composition of sulfate over Phanerozoic time. Shading indicates the kriged 1σ confidence intervals. **(c)** All compiled proxy data for the $\delta^{34}S$ of Phanerozoic seawater.

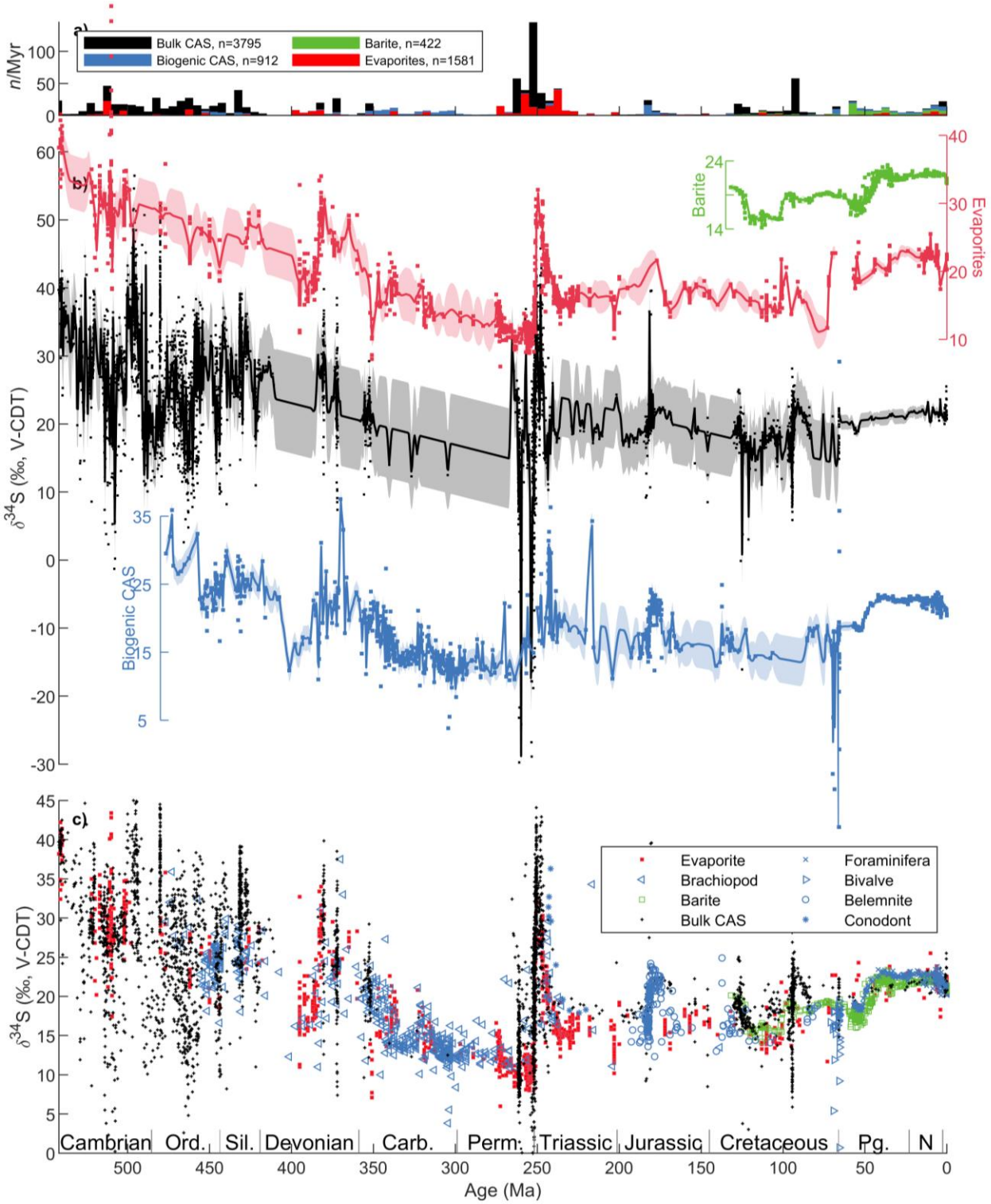
a)
Bulk CAS, n=3795
Biogenic CAS, n=912
Barite, n=422
Evaporites, n=1581
n/Myr
b)
Barite
Evaporites
Biogenic CAS
δ34S (‰, V-CDT)
c)
Evaporite
Brachiopod
Barite
Bulk CAS
Foraminifera
Bivalve
Belemnite
Conodont
δ34S (‰, V-CDT)
Cambrian
Ord.
Sil.
Devonian
Carb.
Perm.
Triassic
Jurassic
Cretaceous
Pg.
N
Age (Ma)

3 Discussion

3.1 Trends and distribution of $\delta^{34}S$ in proxies

During seventy years of effort to determine a history of Phanerozoic seawater sulfate $\delta^{34}S$ from different geologic materials, it has implicitly been assumed that each proxy samples the same primary population of seawater $\delta^{34}S$ compositions through space and time. This is reasonable because Phanerozoic seawater likely contained abundant sulfate as a conservative, well-mixed anion. Modern seawater has 28 mM sulfate, which has an approximate residence time of more than 10 Myr—much longer than the mixing time of the oceans (Bottrell & Newton, 2006; Walker, 1986). The episodic presence of supergiant gypsum and anhydrite deposits in the sedimentary record indicates that sulfate has been a major constituent in ancient seawater, as well. These deposits, which represent long-lived intervals of basin recharge and evaporation of seawater (Warren, 2010), formed episodically from Mesoproterozoic through Phanerozoic time (Grotzinger & Kasting, 1993; Pope & Grotzinger, 2003) during intervals with favorable tectonic and climatic arrangements (Warren, 2010). The composition of fluid inclusions in halite from these evaporite deposits further suggest that sulfate maintained at least millimolar concentrations throughout Phanerozoic time (Lowenstein et al., 2003).

However, comparison of all Phanerozoic $\delta^{34}S$ data for each proxy indicates that the four datasets do not come from the same distribution (Supporting Information, non-parametric Kruskal-Wallis one-way analysis of variance, $\chi^2[3,6709] = 684.54$, $p \ll 0.001$). Therefore, each proxy likely has different temporally or spatially variable sampling biases or reflects different biogeochemical processes that create variance in the time-series of ancient sulfate's $\delta^{34}S$.

All archives exhibit high $\delta^{34}S$ values in early Paleozoic time, fall to minima in the late Paleozoic, and increase to modern values (~21‰) over Mesozoic and Cenozoic time (Figure 1c). This pattern was originally noted in the evaporite record by Ault and Kulp (1959), reaffirmed by more extensive evaporite compilations (Claypool et al., 1980; Holser et al., 1989; Holser & Kaplan, 1966; Strauss, 1997), and confirmed in the CAS record by Kampschulte and Strauss (2004). The $\delta^{34}S$ pattern covaries with many other geochemical records of changing seawater composition (Hannisdal & Peters, 2011; Prokoph et al., 2008), and so has been interpreted to reflect long-term changes in sea-level related to the assembly and breakup of Pangea (Alexandra V. Turchyn & DePaolo, 2019). How changes in tectonic processes directly affect the $\delta^{34}S$ value of seawater sulfate or indirectly affect sulfur mass balance and depositional and diagenetic processes remains unclear (Fike et al., 2015; Alexandra V. Turchyn & DePaolo, 2019).

Seawater sulfate concentrations and $\delta^{34}S$ may have varied on short timescales. Limited periods of sulfate drawdown may coincide with intervals of biogeochemical changes, and these may be expressed as high spatial and temporal $\delta^{34}S$ gradients (Holser, 1977; Kah et al., 2004, 2016). If these gradients represent globally relevant budgets of carbon, nutrients,

and oxidizing capacity, then the residence time of sulfate in ancient oceans must have been much shorter than today, indicating ancient marine sulfate inventories dramatically smaller than the modern inventory or much larger fluxes. For example, the biological pump—remineralization of sinking organic matter that is fractionated by tens of permille from dissolved inorganic carbon—is only capable of creating inorganic carbon isotopic gradients of less than 3‰ given Quaternary nutrient inventories and *ca.* 2 mmol/kg bicarbonate (Toggweiler & Sarmiento, 1985). Fractionations between oxidized and reduced species are comparable for carbon and sulfur, so even small gradients in the $\delta^{34}S$ of marine sulfate, of similar magnitude to carbon isotope gradients driven by the biological pump, would have required both a higher proportion of anaerobic organic carbon remineralization and more than an order of magnitude smaller sulfate inventory.

Two higher-order fluctuations in the evaporite record in the Upper Devonian and the lower Triassic were identified by Holser (1977) and are recorded by CAS as well. Additional fluctuations in the bulk CAS, biogenic CAS, and barite records are apparent due to their higher temporal resolution than the evaporite record for much of the Phanerozoic. In general, the interpolated CAS and barite $\delta^{34}S$ records are within about 10‰ of that of the evaporite record (Figure 2a), suggesting that the other proxy materials record the same first order features of the Phanerozoic sulfur cycle. Which higher-frequency variations reflect spatial or temporal changes in the $\delta^{34}S$ of ancient oceans, and which reflect local or diagenetic controls on the formation of the archive?

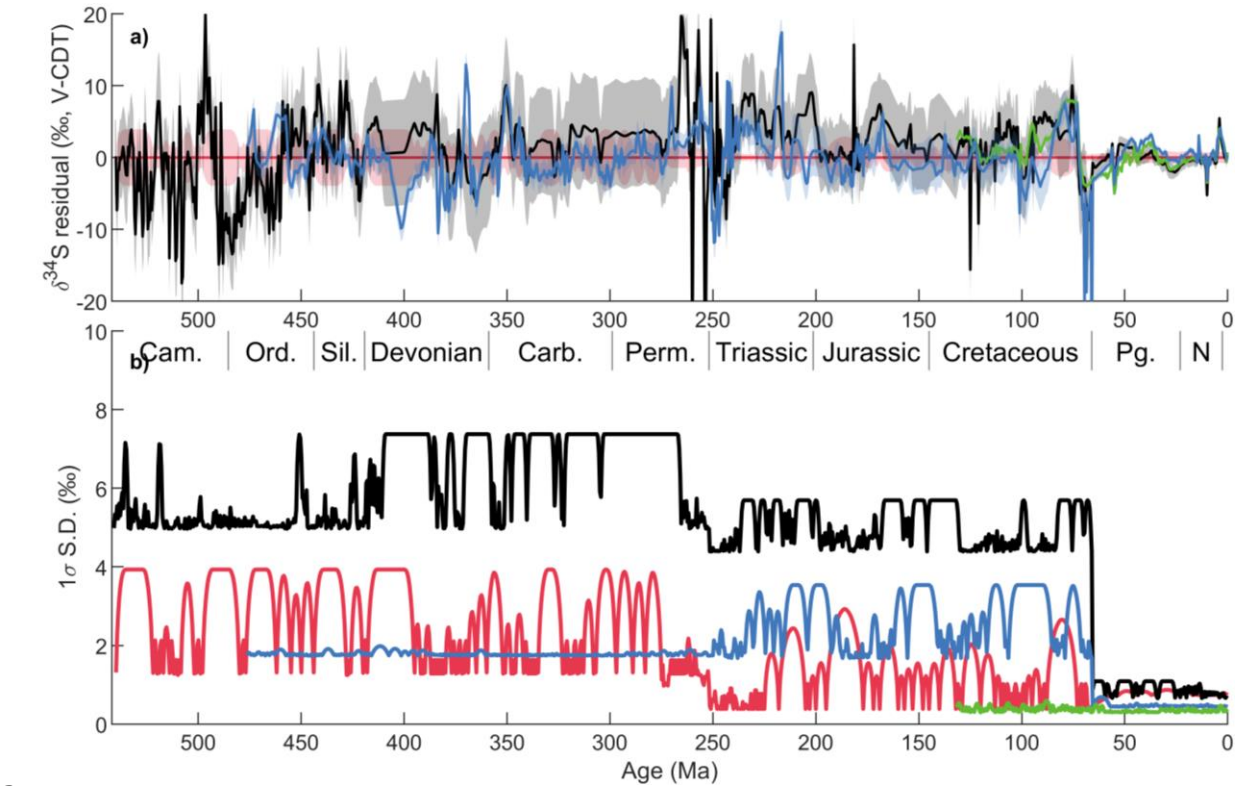

Figure 2. Comparison of $\delta^{34}S$ values and variance generated from proxy materials. **(a)** Residuals between the evaporite record and each other record shaded with kriged 1σ confidence intervals. **(b)** Confidence intervals produced from kriging data from each proxy in each era. Where data is sparse, the confidence intervals approach the standard deviation of linearly detrended data in each geologic period, excluding 1st and 99th percentile outliers. Where there is data, the confidence interval is the uncorrelated chatter determined from the semivariance of data temporally closer than the mean minimum time between data pairs.

3.2 Sources of $\delta^{34}S$ variance

The range of variance for each proxy is plotted in Figure 2b. The maxima in each era on each curve represents the standard deviation of $\delta^{34}S$ data over each geologic era. For example, the standard deviation of linearly detrended Paleozoic bulk CAS data is 7.4‰ (excluding 1st and 99th percentile outliers), while that of all Cenozoic barite data is 1.3‰. These standard deviations reflect the combination of local spatiotemporal trends in seawater sulfate's $\delta^{34}S$, plus an uncorrelated random component. The uncorrelated, random component can be estimated by the semivariance of pairs of data that are closer together than the mean minimum time between all pairs of data (Gebbers, 2010). The uncorrelated variance for each proxy is plotted as the minima in each era on each curve in Figure 2b and represent a measure of the quality of the archives.

The uncorrelated variance is different for each archive and increases with age. Cenozoic and Mesozoic CAS data have uncorrelated variance larger than that of evaporites and barite. Uncorrelated Paleozoic bulk rock CAS data have a standard deviation more than twice that of biogenic CAS and evaporites. This difference between multiple proxies of the same age indicates that the uncorrelated variance is likely caused, in part, by variability inherent to how $\delta^{34}S$ is preserved, rather than just inadequate sampling of primary spatial and temporal variability of seawater sulfate.

The remaining analysis considers the biogeochemical sources of variance in each archive that may have contributed to the uncorrelated variance. Importantly, trends statistically distinguishable from the uncorrelated variance need not represent true trends in the $\delta^{34}S$ of Phanerozoic seawater. The same sources of variance controlling the uncorrelated data may themselves have spatial or temporal components that lead to biased estimates of Phanerozoic seawater's composition in the proxy records. The uncorrelated variance, in part, quantifies the disagreement between contemporaneous records from different localities. Trends in the data smaller than the uncorrelated variance are indistinguishable from random noise. This is true even for individual records from stratigraphic successions with coherent $\delta^{34}S$ trends: a given stratigraphic succession may clearly resolve a trend in the $\delta^{34}S$ of the proxy but fail to statistically resolve a trend in the $\delta^{34}S$ of seawater sulfate.

3.2.1 Evaporites

Deposits of carbonate, sulfate, and halide salts form as seawater evaporates in restricted basins. Throughout Phanerozoic time, bedded marine evaporites formed subaqueously, in salinas (hypersaline lagoons) and salt pans, and subaerially, in supratidal sabkha environments. Extremely thick (>100s of meters) evaporite deposits have also formed in deeper-water environments. Deposition and preservation of evaporites require favorable climatic and tectonic conditions where restricted basins experience net evaporation (Warren, 2010). Therefore, the evaporite record has limited spatial and temporal continuity (Claypool et al., 1980; Strauss, 1997).

Because evaporites are massive products of seawater sulfate, they are largely expected to provide an accurate proxy for the $\delta^{34}S$ of ancient seawater sulfate. However, because they form in marginal marine environments often with biologically adverse salinities, it can be difficult to constrain their geologic age with biostratigraphy. In many deposits, it is also challenging to discern depositional environment or deconvolve marine and non-marine geochemical signatures (Hardie, 1984; Kendall & Harwood, 1989; Lu & Meyers, 2003). The restricted, marginal marine settings in which many evaporites form are prone to changes in fluid source or depositional environment with minor base-level changes (Playà et al., 2007). Basins rich in evaporites also often form diapirs that drive salt tectonics, which complicates a deposit's internal stratigraphy (Nielsen, 1989).

Evaporites can have a $\delta^{34}S$ range of 1‰ to 6‰ within a formation (Thode & Monster, 1965). This variability cannot be attributed to fractionation during gypsum precipitation,

250 which produces sulfate salt prior to halite saturation that has a $\delta^{34}S$ composition 1‰ to 2‰
251 higher than the unevaporated seawater (Raab & Spiro, 1991). Salinity stratification in
252 evaporating basins can promote water-column anoxia and allows MSR to distill sulfate to
253 higher $\delta^{34}S$ compositions than the original seawater; in some cases, evaporite $\delta^{34}S$
254 compositions are higher than other proxies from the same depositional basin (Fike &
255 Grotzinger, 2010). Consequently, early workers hypothesized that the isotopic composition
256 of ancient seawater was best reflected by the lowest $\delta^{34}S$ value in an evaporite succession
257 (Ault & Kulp, 1959; Davies & Krouse, 1975; Thode & Monster, 1965). However,
258 evaporite basins in marginal marine environments are recharged not only by unadulterated
259 seawater, but by groundwater and runoff as well. These fluids may contain sulfate with
260 dramatically different $\delta^{34}S$ compositions from remobilized older evaporite deposits or
261 weathered sedimentary pyrite and organic sulfur (Nielsen & Ricke, 1964; Utrilla et al.,
262 1992). Finally, high organic carbon concentrations in many evaporite deposits can promote
263 isotope fractionation by thermochemical sulfate reduction during burial diagenesis
264 (Vinogradov, 2007).

265 At least some of the uncorrelated variance in evaporite isotope ratio data also results from
266 poor stratigraphic control (Supporting Information). Here we used updated stratigraphic
267 information to better constrain the age of evaporite data, but the record can further benefit
268 from improved resampling during intervals where $\delta^{34}S$ changes appear in other records.
269 Modern stratigraphic models permit relation of evaporite deposition to better age
270 constraints in carbonate and clastic strata. Bernasconi et al. (2017) recently produced a
271 high-resolution evaporite record that resolved the major early Triassic $\delta^{34}S$ excursions seen
272 in earlier datasets; thus careful correlation and assignment of geologic ages permits
273 tracking changes in the Phanerozoic sulfur cycle with evaporites. Indeed, the stratigraphic
274 control for Mesozoic evaporites provided by Bernasconi et al. (2017) likely drives the low
275 standard deviation of uncorrelated Mesozoic evaporite data to values (0.4‰) comparable to
276 that of the marine barite record (0.3‰).

277 3.2.2 Barite

278 Barite precipitates from hydrothermal fluids, sediment pore fluids, and from particles
279 within the marine water column (Paytan et al., 1993, 2002). Barite is under-saturated in
280 most of the ocean (Chow & Goldberg, 1960; Church & Wolgemuth, 1972). However,
281 marine barite has been observed in sediment traps in the upper 200 m in the water column,
282 especially in high-productivity regions, and is associated with sulfate enrichment from
283 decaying organic matter and barite enrichment in dissolving siliceous plankton (Bishop,
284 1988). While barite super-saturation is achieved predominately by the addition of sulfate
285 from oxidizing organic sulfur (Horner et al., 2017; Jacquet et al., 2007), marine barite
286 apparently precipitates with $\delta^{34}S$ values within 0.4‰ of modern seawater (Paytan et al.,
287 1998, 2002). Barite is subsequently transported to sediments by fecal pellets and marine
288 snow (Bishop, 1988), and preserved in oxic marine sediments in high-productivity regions
289 where enough barite is delivered to saturate pore fluids (Church & Wolgemuth, 1972).
290 Sulfate reduction in anoxic sediments can cause dissolution of barite, which re-precipitates

at the base of the sulfate reduction zone with extremely high $\delta^{34}S$ compositions (M. E. Torres et al., 1996).

Marine barite is considered an accurate proxy for ancient seawater $\delta^{34}S$ because it precipitates in the open-ocean water column and is texturally distinguishable from diagenetic barite that forms in anoxic sediments at redox fronts (Paytan et al., 1993). However, the marine barite record is limited by the availability of open-marine sediments that deposited in high-productivity regions wherein authigenic enrichment of barite occurs and where pore fluid sulfate concentrations remain above zero (Paytan et al., 1993). Consequently, the barite $\delta^{34}S$ record is unlikely to be extended much further than the current dataset spanning the last 130 Myr. Paleozoic bedded barite deposits are associated with economically-important metal sulfide deposits (C. A. Johnson et al., 2009), but contain large $\delta^{34}S$ variability (>10‰) and do not resolve the ancient seawater record any better than other proxy materials. Additionally, with few exceptions (e.g., Yao et al., 2018), the temporal resolution of the marine barite $\delta^{34}S$ record is unlikely to dramatically improve, especially during biogeochemical events characterized by low marine productivity (such as the Cretaceous-Paleogene boundary) or bottom-water anoxia (such as ocean anoxic events) that would have limited authigenic barite enrichment or preservation.

3.2.3 Carbonate-associated sulfate

Limestones and dolomites were deposited continuously throughout Phanerozoic time, accumulating in marginal marine and open-ocean environments. A minor amount of sulfate is incorporated into biogenic and abiogenic carbonate phases. Biogenic carbonates often contain part-per-thousand sulfate by mass, while inorganic cements typically contain hundreds of parts-per-million (Barkan et al., 2020; Busenberg & Plummer, 1985; Giri & Swart, 2019; Paris, Fehrenbacher, et al., 2014; Staudt & Schoonen, 1995). Recent sediments from various peritidal carbonate platform environments include CAS with an isotopic composition similar to modern seawater (Lyons et al., 2004). CAS, therefore, complements and exceeds the temporal resolution and completeness of the evaporite and barite records (Strauss, 1997).

Diagenetic processes may exchange sulfate with the primary carbonate and alter its isotopic composition (Fichtner et al., 2017; Present et al., 2015, 2019). Kampschulte & Strauss (2004) suggested that the variability of multiple $\delta^{34}S$ analyses from contemporaneous stratigraphic successions could be used to quantify the effect of diagenesis on the CAS record. However, rapidly-changing and disparate CAS $\delta^{34}S$ compositions have since been generated and interpreted—especially in Paleozoic studies—as intervals of heterogeneous seawater sulfate $\delta^{34}S$ reflecting periods of low sulfate concentrations and low marine sulfate residence times (e.g., Gill, Lyons, Young, et al., 2011; Kah et al., 2004).

Limestones and dolomites are comprised of mud or grains that precipitated both biologically and abiotically from seawater, with cements binding them together. Each of these components may recrystallize in pore fluids whose chemical composition reflects

marine, meteoric, and burial diagenetic processes. A combustion CAS analysis typically requires 10 g to 100 g of carbonate (Wotte et al., 2012), and this mass requirement dictates that samples mix components that may have precipitated and/or recrystallized at different times. Recent application of plasma-source mass spectrometry for sulfur isotope analysis has permitted $\delta^{34}S$ analyses on less than one-thousandth as much sulfate, corresponding to 5 mg to 50 mg of carbonate (Paris, Adkins, et al., 2014; Paris et al., 2013; Present et al., 2015, 2019; Rennie et al., 2018). Well-preserved biogenic grains, recrystallized grains, matrix, and cements contain CAS with $\delta^{34}S$ compositions varying by as much as 25‰, spanning most of range of CAS analyses from the entire Phanerozoic (Present et al., 2015, 2019). Therefore, much of the variability of CAS $\delta^{34}S$ data may not reflect the $\delta^{34}S$ composition of ancient seawater sulfate. Identifying components that retain the $\delta^{34}S$ of sulfate incorporated from syndepositional seawater is critical to precisely and accurately exploit the CAS $\delta^{34}S$ archive.

CAS can reflect the $\delta^{34}S$ of syndepositional seawater sulfate if the carbonate component did not recrystallize after precipitation, if recrystallization and cementation occurred in contact with a low-sulfate fluid, or if the $\delta^{34}S$ of pore fluid sulfate was not fractionated from seawater (Gill et al., 2008; Lyons et al., 2004; Rennie & Turchyn, 2014). Alteration occurs if the sediments recrystallize above the depth at which sulfate is completely consumed by MSR but deep enough that some distillation of $\delta^{34}S$ within sediment pore fluid has occurred (Fike et al., 2015; Present et al., 2019; Rennie & Turchyn, 2014; Witts et al., 2018). Additionally, some ancient carbonates contain CAS with anomalously low $\delta^{34}S$ interpreted to result from the incorporation of sulfate from sulfide that was reoxidized during diagenesis or weathering (Baldermann et al., 2015; Fichtner et al., 2017; Fike et al., 2015; P. J. Marenco et al., 2008; Present et al., 2015, 2019; Rennie & Turchyn, 2014; Riccardi et al., 2006; Yan et al., 2013). Carbonates recrystallizing during burial may also be prone to diagenetic modification of the $\delta^{34}S$ of CAS if the burial fluids were sulfate rich (Fichtner et al., 2017, 2018; Present et al., 2015). The $\delta^{34}S$ in burial fluids may be highly variable, and include sulfate from hydrocarbon or organic matter degradation (Fichtner et al., 2018; Thode & Monster, 1965, 1970), dissolved evaporites, or groundwater modified by MSR (Dogramaci et al., 2001; Present et al., 2019).

These diagenetic controls on the $\delta^{34}S$ of CAS decrease the precision and accuracy of the proxy. This is quantified by its uncorrelated variance, which is much higher in the CAS archive than that observed in other seawater sulfate $\delta^{34}S$ proxies. Uncorrelated Paleozoic CAS data has a standard deviation of 5.0‰, and that of Mesozoic CAS is 4.4‰, which is five to ten times larger than that of Paleozoic and Mesozoic evaporites (1.0‰ and 0.4‰, respectively). Further, diagenesis may have impacted accuracy by systematically biasing the $\delta^{34}S$ of CAS with respect to the primary composition of seawater sulfate. For example, base level often controls the stratigraphic arrangement of facies in carbonates successions, which can impart biases as large as 10‰ on the $\delta^{34}S$ of CAS (Present et al., 2019; Richardson et al., 2019). Both the random and systematic variability is on the order of well-resolved rapid changes of 3‰ to 6‰ in the $\delta^{34}S$ of marine barite and biogenic CAS.

3.2.4 Biogenic CAS

Biogenic CAS may offer a more robust $\delta^{34}S$ record than bulk CAS because biogenic carbonate can often be readily separated from other limestone components, preservation quality can be assessed, and vital effects appear to be small in most taxa (A. Kampschulte et al., 2001; Paris, Fehrenbacher, et al., 2014; Present et al., 2015). In modern and cultured biogenic carbonates, the incorporated sulfate has an isotopic composition within 2‰ of the seawater from which it precipitated (Burdett et al., 1989; A. Kampschulte et al., 2001; Kaplan et al., 1963; Mekhtiyeva, 1974; Paris et al., 2013; Paris, Fehrenbacher, et al., 2014; Present et al., 2015). Burdett et al. (1989) produced the first continuous biogenic CAS dataset for the Neogene Period and demonstrated that it agreed with the evaporite $\delta^{34}S$ record. Kampschulte et al. (2001) and Kampschulte and Strauss (2004) then demonstrated that biogenic CAS captured the first-order features of the Phanerozoic evaporite record, and could be correlated with higher resolution and confidence than evaporites to the carbonate carbon isotope record. More recently, Rennie et al. (2018) produced a taxon-specific foraminiferal CAS record with variance and secular trends comparable to the marine barite record.

Low-magnesium calcite, precipitated by many brachiopods, belemnites, and planktonic foraminifera, is stable at Earth's surface and shallow burial conditions. The low-magnesium calcite biogenic CAS $\delta^{34}S$ record has significantly improved the resolution of the Phanerozoic $\delta^{34}S$ record during two key periods. First, during the Toarcian (Jurassic) Ocean Anoxic Event, belemnite CAS displays a large (6‰) $\delta^{34}S$ excursion that is not apparent in the evaporite record (Gill, Lyons, & Jenkyns, 2011; Newton et al., 2011). Second, during Carboniferous time, brachiopods record a prolonged recovery from a $\delta^{34}S$ maximum in middle Devonian time (D. J. Johnson et al., in revision; A. Kampschulte et al., 2001; N. Wu et al., 2014). However, aragonite and high-magnesium calcite, precipitated by many bivalves, gastropods, corals, trilobites, echinoderms, bryozoans, and marine algae, commonly dissolves and/or recrystallizes to calcite or dolomite during burial (Brand & Veizer, 1980). Few studies have investigated CAS $\delta^{34}S$ from formerly aragonitic fossils (Mekhtiyeva, 1974; Present et al., 2015; Witts et al., 2018).

Unfortunately, well-preserved biogenic carbonate is rare in the rock record, especially during intervals of climatic or biologic crisis (e.g., mass extinction events). Even apparently well-preserved biogenic carbonate can still be susceptible to diagenetic alteration (Fichtner et al., 2018; Witts et al., 2018). Like the marine barite record, a significant expansion of the biogenic CAS $\delta^{34}S$ proxy record is limited by the availability of suitable sample material.

3.3 Discrepant early Phanerozoic proxy records

Major $\delta^{34}S$ trends and excursions in Cenozoic, Mesozoic, and late Paleozoic records are exhibited in multiple archives, but significant discrepancies and gaps are apparent in records from Cambrian to Devonian time (Figure 1c). In early- to mid-Paleozoic strata,

biogenic carbonates are sparse, marine barite is absent, and bulk CAS $\delta^{34}S$ values diverge from evaporites by greater than 10‰ (Figure 2a). Additionally, Paleozoic variance is highest for all records (Figure 2b). New approaches are necessary to better resolve the structure of early- to mid-Paleozoic seawater sulfate $\delta^{34}S$.

Large $\delta^{34}S$ excursions correlate with global perturbations evidenced by carbon isotope excursions and trace metal, pyrite sulfur isotope, and bioturbation intensity records (Canfield & Farquhar, 2009; Fike et al., 2015; Gill et al., 2007; Jones & Fike, 2013). Because part of the $\delta^{34}S$ variance in all archives derives from depositional and early diagenetic processes—such as MSR, pyrite formation, and sulfide reoxidation—careful attention to facies and depositional controls may reveal important changes in organic matter and metal cycling in marine pore fluids (Fike & Grotzinger, 2010; Present et al., 2019; Rennie & Turchyn, 2014; Richardson et al., 2019). Embracing the information content in the spatial and temporal structure of these sources of variance should enrich understanding of Paleozoic oceanographic, biologic, and climatic change.

4 Conclusions

Phanerozoic $\delta^{34}S$ data were compiled from evaporites, barite, biogenic CAS, and bulk rock CAS and updated to a consistent time scale. Each of these archives contains spatial and temporal biases arising from both syndepositional and diagenetic biogeochemical processes. The variance in each record increases with age, partly due to the increased importance of post-depositional processes in older materials.

The barite record has the lowest variance and likely accurately captures the $\delta^{34}S$ of ancient oceans. However, its spatial and temporal extent is limited to the availability of suitable marine sediment cores. The evaporite record was built from massive amounts of ancient seawater sulfate, and while it can be impacted by processes associated with sulfur cycling in these marginal marine basins, its largest limitation emerges from requirements of favorable climatic and tectonic conditions to form and preserve these basins. Biogenic CAS $\delta^{34}S$ analyses have similar variance to the evaporite record but have a higher temporal resolution. The biogenic CAS record thus appears to resolve marine sulfur cycle features not apparent in other archives during the Carboniferous and the Jurassic. However, $\delta^{34}S$ data from even the best-preserved biogenic carbonate material must be interpreted in the context of additional constraints on the diagenetic history of the sample.

Bulk CAS contains a statistically significant different distribution of $\delta^{34}S$ compositions than the biogenic CAS, evaporite, or barite records. Early diagenetic overprinting of CAS occurs in depositional environments where carbonate recrystallization and cementation coincides with sulfate-rich pore fluids with modified $\delta^{34}S$ values. Despite these complications, bulk CAS can be widely applied in ancient sedimentary basins and is the only archive readily able to resolve sulfur cycle changes during rapid biogeochemical events and to extend the $\delta^{34}S$ record into Precambrian time.

Reconstructing ancient seawater chemistry from sedimentary proxy archives requires assessing primary and diagenetic sources of variance. The comparison of different archives of $\delta^{34}S$ in sedimentary sulfate presented here increases confidence in robust features of the record; this will help guide future interpretation of data from key biogeochemical transitions in the Phanerozoic, and inform interrogation of Precambrian strata for which fewer archives are available.

Acknowledgements

No new data were collected for this study. Datasets compiled for this research are tabulated in the Supplemental Material and referenced below. We thank Caltech DocuServe for obtaining many of the publications containing the compiled data, and John Grotzinger and Joe Kirschvink for thoughtful advising and feedback.

References

Adams, D. D., Hurtgen, M. T., & Sageman, B. B. (2010). Volcanic triggering of a biogeochemical cascade during Oceanic Anoxic Event 2. *Nature Geoscience*, *3*(3), 201–204. https://doi.org/10.1038/Ngeo743

Algeo, T. J., Henderson, C. M., Tong, J., Feng, Q., Yin, H., & Tyson, R. V. (2013). Plankton and productivity during the Permian–Triassic boundary crisis: An analysis of organic carbon fluxes. *Global and Planetary Change*, *105*, 52–67. https://doi.org/10.1016/j.gloplacha.2012.02.008

Arp, G., Ostertag-Henning, C., YÜCekent, S., Reitner, J., & Thiel, V. (2008). Methane-related microbial gypsum calcitization in stromatolites of a marine evaporative setting (Münder Formation, Upper Jurassic, Hils Syncline, north Germany). *Sedimentology*, *55*(5), 1227–1251. https://doi.org/10.1111/j.1365-3091.2007.00944.x

Ault, W. U., & Kulp, J. L. (1959). Isotopic geochemistry of sulphur. *Geochimica et Cosmochimica Acta*, *16*(4), 201–235. https://doi.org/10.1016/0016-7037(59)90112-7

Balderer, W., Pearson, F. J., & Soreau, S. (1991). Formation-Specific Characterization of Groundwaters. In F. J. Pearson, W. Balderer, H. H. Loosli, B. E. Lehmann, A. Matter, T. Peters, et al. (Eds.), *Applied Isotope Hydrogeology: A Case Study in Northern Switzerland: Technical Report 88-01* (pp. 297–374). Amsterdam: Elsevier. Retrieved from https://books.google.com/books?id=fEBs7PudzAEC

Baldermann, A., Deditius, A. P., Dietzel, M., Fichtner, V., Fischer, C., Hippler, D., et al. (2015). The role of bacterial sulfate reduction during dolomite precipitation: Implications from Upper Jurassic platform carbonates. *Chemical Geology*, *412*, 1–14. https://doi.org/10.1016/j.chemgeo.2015.07.020

Barkan, Y., Paris, G., Webb, S. M., Adkins, J. F., & Halevy, I. (2020). Sulfur isotope fractionation between aqueous and carbonate-associated sulfate in abiotic calcite and aragonite. *Geochimica et Cosmochimica Acta*. https://doi.org/10.1016/j.gca.2020.03.022

Ben-Yaakov, S. (1973). pH Buffering of Pore Water of Recent Anoxic Marine Sediments. *Limnology and Oceanography*, *18*(1), 86–94. https://doi.org/10.4319/lo.1973.18.1.0086

Berggren, W. A., Kent, D. V., Flynn, J. J., & Van Couvering, J. A. (1985). Cenozoic geochronology. *Geological Society of America Bulletin*, *96*, 1407–1418.

Berggren, W. A., Kent, D. V., Swisher, C. C., & Aubry, M.-P. (1995). A Revised Cenozoic Geochronology and Chronostratigraphy. In *Geochronology, Time Scales and Global Stratigraphic Correlation* (pp. 129–212). SEPM (Society for Sedimentary Geology). https://doi.org/10.2110/pec.95.04.0129

Bergström, S. M., Chen, X., Gutiérrez-Marco, J. C., & Dronov, A. (2009). The new chronostratigraphic classification of the Ordovician System and its relations to major regional series and stages and to δ13C chemostratigraphy. *Lethaia*, *42*(1), 97–107. https://doi.org/10.1111/j.1502-3931.2008.00136.x

Bernasconi, S. M., Meier, I., Wohlwend, S., Brack, P., Hochuli, P. A., Bläsi, H., et al. (2017). An evaporite-based high-resolution sulfur isotope record of Late Permian and Triassic seawater sulfate. *Geochimica et Cosmochimica Acta*, *204*, 331–349. https://doi.org/10.1016/j.gca.2017.01.047

Bishop, J. K. B. (1988). The barite-opal-organic carbon association in oceanic particulate matter. *Nature*, *332*(6162), 341–343. https://doi.org/10.1038/332341a0

Blomquist, P. K. (2016). Wolfcamp Horizontal Play, Midland Basin, West Texas, #10890 (2016). In *AAPG Pacific Section and Rocky Mountain Section Joint Meeting* (p. 34). Las Vegas, Nevada. Retrieved from http://www.searchanddiscovery.com/pdfz/documents/2016/10890blomquist/ndx_blomquist.pdf.html

Boschetti, T., Cortecchi, G., Toscani, L., & Iacumin, P. (2011). Sulfur and oxygen isotope compositions of Upper Triassic sulfates from Northerm Apennines (Italy): palaeogeographic and hidrogeochemical implications. *Geologica Acta*, *9*(2), 129–147. https://doi.org/10.1344/105.000001690

Bottrell, S. H., & Newton, R. J. (2006). Reconstruction of changes in global sulfur cycling from marine sulfate isotopes. *Earth-Science Reviews*, *75*(1–4), 59–83. https://doi.org/10.1016/j.earscirev.2005.10.004

Bowles, M. W., Mogollón, J. M., Kasten, S., Zabel, M., & Hinrichs, K.-U. (2014). Global rates of marine sulfate reduction and implications for sub–sea-floor metabolic activities. *Science*, *344*(6186), 889. https://doi.org/10.1126/science.1249213

Bowring, S. A., Erwin, D. H., Jin, Y. G., Martin, M. W., Davidek, K., & Wang, W. (1998). U/Pb Zircon Geochronology and Tempo of the End-Permian Mass Extinction. *Science*, *280*(5366), 1039–1045. https://doi.org/10.1126/science.280.5366.1039

Brand, U., & Veizer, J. (1980). Chemical diagenesis of a multicomponent carbonate system; 1, Trace elements. *Journal of Sedimentary Research*, *50*(4), 1219–1236. https://doi.org/10.1306/212f7bb7-2b24-11d7-8648000102c1865d

Burdett, J. W., Arthur, M. A., & Richardson, M. (1989). A Neogene seawater sulfur isotope age curve from calcareous pelagic microfossils. *Earth and Planetary Science Letters*, *94*, 189–198. https://doi.org/10.1016/0012-821x(89)90138-6

Burgess, S. D., Bowring, S., & Shen, S. (2014). High-precision timeline for Earth's most severe extinction. *Proceedings of the National Academy of Sciences*. https://doi.org/10.1073/pnas.1317692111

Burke, A., Present, T. M., Paris, G., Rae, E. C. M., Sandilands, B. H., Gaillardet, J., et al. (2018). Sulfur isotopes in rivers: Insights into global weathering budgets, pyrite oxidation, and the modern sulfur cycle. *Earth and Planetary Science Letters*. https://doi.org/10.1016/j.epsl.2018.05.022

Buschendorf, Fr., Nielsen, H., Puchelt, H., & Ricke, W. (1963). Schwefel-Isotopen-Untersuchungen am Pyrit-Sphalerit-Baryt-Lager Meggen/Lenne (Deutschland) und an verschiedenen Devon-Evaporiten. *Geochimica et Cosmochimica Acta*, *27*(5), 501–523. https://doi.org/10.1016/0016-7037(63)90085-1

Busenberg, E., & Plummer, N. L. (1985). Kinetic and thermodynamic factors controlling the distribution of SO42− and Na+ in calcites and selected aragonites. *Geochimica et Cosmochimica Acta*, *49*(3), 713–725. https://doi.org/10.1016/0016-7037(85)90166-8

Cai, C., Hu, W., & Worden, R. H. (2001). Thermochemical sulphate reduction in Cambro–Ordovician carbonates in Central Tarim. *Marine and Petroleum Geology*, *18*(6), 729–741. https://doi.org/10.1016/S0264-8172(01)00028-9

Canfield, D. E., & Farquhar, J. (2009). Animal evolution, bioturbation, and the sulfate concentration of the oceans. *Proceedings of the National Academy of Sciences*, *106*(20), 8123–8127. https://doi.org/10.1073/pnas.0902037106

Chen, D., Wang, J., Racki, G., Li, H., Wang, C., Ma, X., & Whalen, M. T. (2013). Large sulphur isotopic perturbations and oceanic changes during the Frasnian–Famennian transition of the Late Devonian. *Journal of the Geological Society*, *170*(3), 465–476. https://doi.org/10.1144/jgs2012-037

Chen, J., Zhao, R., Huo, W., Yao Yuyuan Pan, S., Shao, M., & Hai, C. (1981). Sulfur Isotopes of Some Marine Gypsum. *Chinese Journal of Geology*, *3*, 009.

Chow, T. J., & Goldberg, E. D. (1960). On the marine geochemistry of barium. *Geochimica et Cosmochimica Acta*, *20*(3), 192–198. https://doi.org/10.1016/0016-7037(60)90073-9

Church, T. M., & Wolgemuth, K. (1972). Marine barite saturation. *Earth and Planetary Science Letters*, *15*(1), 35–44. https://doi.org/10.1016/0012-821X(72)90026-X

Claypool, G. E., Holser, W. T., Kaplan, I. R., Sakai, H., & Zak, I. (1980). The age curves of sulfur and oxygen isotopes in marine sulfate and their mutual interpretation. *Chemical Geology*, *28*, 199–260. https://doi.org/10.1016/0009-2541(80)90047-9

Cohen, K., Finney, S., Gibbard, P., & Fan, J.-X. (2013). The ICS international chronostratigraphic chart. *Episodes*, *36*(3), 199–204.

Cortecci, G., Reyes, E., Berti, G., & Casati, P. (1981). Sulfur and oxygen isotopes in Italian marine sulfates of Permian and Triassic ages. *Chemical Geology*, *34*(1), 65–79. https://doi.org/10.1016/0009-2541(81)90072-3

Cramer, B. D., Loydell, D. K., Samtleben, C., Munnecke, A., Kaljo, D., Männik, P., et al. (2010). Testing the limits of Paleozoic chronostratigraphic correlation via high-resolution (<500 k.y.) integrated conodont, graptolite, and carbon isotope (δ13Ccarb) biochemostratigraphy across the Llandovery–Wenlock (Silurian) boundary: Is a unified Phanerozoic time scale achievable? *Geological Society of America Bulletin*, 17.

Cramer, B. D., Condon, D. J., Söderlund, U., Marshall, C., Worton, G. J., Thomas, A. T., et al. (2012). U-Pb (zircon) age constraints on the timing and duration of Wenlock

(Silurian) paleocommunity collapse and recovery during the "Big Crisis." *GSA Bulletin*, *124*(11–12), 1841–1857. https://doi.org/10.1130/B30642.1

Dahl, T. W., Connelly, J. N., Li, D., Kouchinsky, A., Gill, B. C., Porter, S., et al. (2019). Atmosphere–ocean oxygen and productivity dynamics during early animal radiations. *Proceedings of the National Academy of Sciences*, *116*(39), 19352–19361. https://doi.org/10.1073/pnas.1901178116

Das, N., Horita, J., & Holland, H. D. (1990). Chemistry of fluid inclusions in halite from the Salina Group of the Michigan basin: Implications for Late Silurian seawater and the origin of sedimentary brines. *Geochimica et Cosmochimica Acta*, *54*(2), 319–327. https://doi.org/10.1016/0016-7037(90)90321-B

Davies, G. R., & Krouse, H. R. (1975). Sulphur isotope distribution in Paleozoic sulphate evaporites, Canadian Arctic Archipelago. *Geological Survey of Canada Paper*, *75–1 Part B*, 221–225.

Dogramaci, S. S., Herczeg, A. L., Schiff, S. L., & Bone, Y. (2001). Controls on δ34S and δ18O of dissolved sulfate in aquifers of the Murray Basin, Australia and their use as indicators of flow processes. *Applied Geochemistry*, *16*(4), 475–488. https://doi.org/10.1016/S0883-2927(00)00052-4

Edwards, C. T., Fike, D. A., Saltzman, M. R., Lu, W., & Lu, Z. (2018). Evidence for local and global redox conditions at an Early Ordovician (Tremadocian) mass extinction. *Earth and Planetary Science Letters*, *481*, 125–135. https://doi.org/10.1016/j.epsl.2017.10.002

van Everdingen, R. O., Shakur, M. A., & Krouse, H. R. (1982). 34S and 18O abundances differentiate Upper Cambrian and Lower Devonian gypsum-bearing units, District of Mackenzie, N.W.T.—an update. *Canadian Journal of Earth Sciences*, *19*(6), 1246–1254. https://doi.org/10.1139/e82-106

Fanlo, I., & Ayora, C. (1998). The evolution of the Lorraine evaporite basin: implications for the chemical and isotope composition of the Triassic ocean. *Chemical Geology*, *146*(3), 135–154. https://doi.org/10.1016/S0009-2541(98)00007-2

Feely, H. W., & Kulp, J. L. (1957). Origin of Gulf Coast Salt-Dome Sulphur Deposits. *AAPG Bulletin*, *41*(8), 1802–1853.

Fichtner, V., Strauss, H., Immenhauser, A., Buhl, D., Neuser, R. D., & Niedermayr, A. (2017). Diagenesis of carbonate associated sulfate. *Chemical Geology*, *463*(Supplement C), 61–75. https://doi.org/10.1016/j.chemgeo.2017.05.008

Fichtner, V., Strauss, H., Mavromatis, V., Dietzel, M., Huthwelker, T., Borca, C. N., et al. (2018). Incorporation and subsequent diagenetic alteration of sulfur in Arctica islandica. *Chemical Geology*, *482*, 72–90. https://doi.org/10.1016/j.chemgeo.2018.01.035

Fike, D. A., & Grotzinger, J. P. (2008). A paired sulfate–pyrite δ34S approach to understanding the evolution of the Ediacaran–Cambrian sulfur cycle. *Geochimica et Cosmochimica Acta*, *72*(11), 2636–2648. https://doi.org/10.1016/j.gca.2008.03.021

Fike, D. A., & Grotzinger, J. P. (2010). A δ34SSO4 approach to reconstructing biogenic pyrite burial in carbonate-evaporite basins: An example from the Ara Group, Sultanate of Oman. *Geology*, *38*, 371–374.

Fike, D. A., Bradley, A. S., & Rose, C. V. (2015). Rethinking the Ancient Sulfur Cycle. *Annual Review of Earth and Planetary Sciences*, *43*(1), 593–622. https://doi.org/10.1146/annurev-earth-060313-054802

Fox, J. S., & Videtich, P. E. (1997). Revised estimate of δ34S for marine sulfates from the Upper Ordovician: data from the Williston Basin, North Dakota, U.S.A. *Applied Geochemistry*, *12*(1), 97–103. https://doi.org/10.1016/S0883-2927(96)00065-0

Froelich, P. N., Klinkhammer, G. P., Bender, M. L., Luedtke, N. A., Heath, G. R., Cullen, D., et al. (1979). Early oxidation of organic matter in pelagic sediments of the eastern equatorial Atlantic: suboxic diagenesis. *Geochimica et Cosmochimica Acta*, *43*, 1075–1090. https://doi.org/10.1016/0016-7037(79)90095-4

Gebbers, R. (2010). Geostatistics and Kriging. In M. H. Trauth, *MATLAB Recipes for Earth Sciences* (3rd Ed., pp. 235–254). Berlin, Germany: Springer-Verlag.

Gill, B. C., Lyons, T. W., & Saltzman, M. R. (2007). Parallel, high-resolution carbon and sulfur isotope records of the evolving Paleozoic marine sulfur reservoir. *Palaeogeography, Palaeoclimatology, Palaeoecology*, *256*, 156–173. https://doi.org/10.1016/j.palaeo.2007.02.030

Gill, B. C., Lyons, T. W., & Frank, T. D. (2008). Behavior of carbonate-associated sulfate during meteoric diagenesis and implications for the sulfur isotope paleoproxy. *Geochimica et Cosmochimica Acta*, *72*, 4699–4711. https://doi.org/10.1016/j.gca.2008.07.001

Gill, B. C., Lyons, T. W., & Jenkyns, H. C. (2011). A global perturbation to the sulfur cycle during the Toarcian Oceanic Anoxic Event. *Earth and Planetary Science Letters*, *312*, 484–496. https://doi.org/10.1016/j.epsl.2011.10.030

Gill, B. C., Lyons, T. W., Young, S. A., Kump, L. R., Knoll, A. H., & Saltzman, M. R. (2011). Geochemical evidence for widespread euxinia in the Later Cambrian ocean. *Nature*, *469*, 80–83.

Giri, S. J., & Swart, P. K. (2019). The influence of seawater chemistry on carbonate-associated sulfate derived from coral skeletons. *Palaeogeography, Palaeoclimatology, Palaeoecology*, *521*, 72–81. https://doi.org/10.1016/j.palaeo.2019.02.011

Gomes, M. L., Hurtgen, M. T., & Sageman, B. B. (2016). Biogeochemical sulfur cycling during Cretaceous oceanic anoxic events: A comparison of OAE1a and OAE2. *Paleoceanography*, *31*(2), 2015PA002869. https://doi.org/10.1002/2015PA002869

Gorjan, P., & Kaiho, K. (2007). Correlation and comparison of seawater δ34Ssulfate records at the Permian-Triassic transition. *Chemical Geology*, *243*, 275–285. https://doi.org/10.1016/j.chemgeo.2007.03.011

Grotzinger, J. P., & Kasting, J. F. (1993). New constraints on Precambrian ocean composition. *The Journal of Geology*, 235–243.

Guo, C., Chen, D., Song, Y., Zhou, X., Ding, Y., & Zhang, G. (2018). Depositional environments and cyclicity of the Early Ordovician carbonate ramp in the western Tarim Basin (NW China). *Journal of Asian Earth Sciences*, *158*, 29–48. https://doi.org/10.1016/j.jseaes.2018.02.006

Handford, C. R., & Dutton, S. P. (1980). Pennsylvanian–Early Permian Depositional Systems and Shelf-Margin Evolution, Palo Duro Basin, Texas. *AAPG Bulletin*, *64*(1), 88–106. https://doi.org/10.1306/2F918932-16CE-11D7-8645000102C1865D

Hannisdal, B., & Peters, S. E. (2011). Phanerozoic Earth System Evolution and Marine Biodiversity. *Science*, *334*(6059), 1121–1124. https://doi.org/10.1126/science.1210695

Hardie, L. A. (1984). Evaporites; marine or non-marine? *American Journal of Science*, *284*(3), 193–240. https://doi.org/10.2475/ajs.284.3.193

Harland, W., Armstrong, R., Cox, A., Craig, L., Smith, A., & Smith, D. (1990). *A Geologic Time Scale 1989*. Cambridge University Press.

Harrison, A. G., & Thode, H. G. (1958). Mechanism of the bacterial reduction of sulphate from isotope fractionation studies. *Transactions of the Faraday Society*, *54*, 84. https://doi.org/10.1039/tf9585400084

He, T., Zhu, M., Mills, B. J. W., Wynn, P. M., Zhuravlev, A. Y., Tostevin, R., et al. (2019). Possible links between extreme oxygen perturbations and the Cambrian radiation of animals. *Nature Geoscience*, 1. https://doi.org/10.1038/s41561-019-0357-z

Hearn, M. R., Machel, H. G., & Rostron, B. J. (2011). Hydrocarbon breaching of a regional aquitard: The Devonian Ireton Formation, Bashaw area, Alberta, Canada. *AAPG Bulletin*, *95*(6), 1009–1037. https://doi.org/10.1306/09271010050

Hitchon, B., & Krouse, H. R. (1972). Hydrogeochemistry of the surface waters of the Mackenzie River drainage basin, Canada—III. Stable isotopes of oxygen, carbon and sulphur. *Geochimica et Cosmochimica Acta*, *36*(12), 1337–1357. https://doi.org/10.1016/0016-7037(72)90066-X

Holland, H. D. (1973). Systematics of the isotopic composition of sulfur in the oceans during the Phanerozoic and its implications for atmospheric oxygen. *Geochimica et Cosmochimica Acta*, *37*(12), 2605–2616. https://doi.org/10.1016/0016-7037(73)90268-8

Holser, W. T. (1977). Catastrophic chemical events in the history of the ocean. *Nature*, *267*, 403–408.

Holser, W. T., & Kaplan, I. R. (1966). Isotope geochemistry of sedimentary sulfates. *Chemical Geology*, *1*, 93–135. https://doi.org/10.1016/0009-2541(66)90011-8

Holser, W. T., Maynard, J. B., & Cruikshank, K. (1989). Modelling the natural cycle of sulphur through Phanerozoic time. *Evolution of the Global Biogeochemical Sulphur Cycle. Wiley, New York*, 21–56.

Horacek, M., Brandner, R., Richoz, S., & Povoden-Karadeniz, E. (2010). Lower Triassic sulphur isotope curve of marine sulphates from the Dolomites, N-Italy. *Palaeogeography, Palaeoclimatology, Palaeoecology*, *290*(1), 65–70. https://doi.org/10.1016/j.palaeo.2010.02.016

Horner, T. J., Pryer, H. V., Nielsen, S. G., Crockford, P. W., Gauglitz, J. M., Wing, B. A., & Ricketts, R. D. (2017). Pelagic barite precipitation at micromolar ambient sulfate. *Nature Communications*, *8*(1), 1342. https://doi.org/10.1038/s41467-017-01229-5

Hovorka, S. D., Knauth, L. P., Fisher, R. S., & Gao, G. (1993). Marine to nonmarine facies transition in Permian evaporites of the Palo Duro Basin, Texas: Geochemical response. *GSA Bulletin*, *105*(8), 1119–1134. https://doi.org/10.1130/0016-7606(1993)105<1119:MTNFTI>2.3.CO;2

Hurtgen, M. T., Pruss, S. B., & Knoll, A. H. (2009). Evaluating the relationship between the carbon and sulfur cycles in the later Cambrian ocean: An example from the Port au

Port Group, western Newfoundland, Canada. *Earth and Planetary Science Letters*, *281*(3–4), 288–297. https://doi.org/10.1016/j.epsl.2009.02.033

Insalaco, E., Virgone, A., Courme, B., Gaillot, J., Kamali, M., Moallemi, A., et al. (2006). Upper Dalan Member and Kangan Formation between the Zagros Mountains and offshore Fars, Iran: depositional system, biostratigraphy and stratigraphic architecture. *GeoArabia*, *11*(2), 75–176.

Jacquet, S. H. M., Henjes, J., Dehairs, F., Worobiec, A., Savoye, N., & Cardinal, D. (2007). Particulate Ba-barite and acantharians in the Southern Ocean during the European Iron Fertilization Experiment (EIFEX). *Journal of Geophysical Research: Biogeosciences*, *112*(G4). https://doi.org/10.1029/2006JG000394

John, E. H., Wignall, P. B., Newton, R. J., & Bottrell, S. H. (2010). δ34SCAS and δ18OCAS records during the Frasnian–Famennian (Late Devonian) transition and their bearing on mass extinction models. *Chemical Geology*, *275*(3–4), 221–234. https://doi.org/10.1016/j.chemgeo.2010.05.012

Johnson, C. A., Emsbo, P., Poole, F. G., & Rye, R. O. (2009). Sulfur- and oxygen-isotopes in sediment-hosted stratiform barite deposits. *Geochimica et Cosmochimica Acta*, *73*(1), 133–147. https://doi.org/10.1016/j.gca.2008.10.011

Johnson, D. J., Grossman, E. L., & Adkins, J. F. (in revision). Single-brachiopod δ34SCAS indicates a dynamic, climate-influenced Permo-Carboniferous S cycle. *Earth and Planetary Science Letters*.

Jones, D. S., & Fike, D. A. (2013). Dynamic sulfur and carbon cycling through the end-Ordovician extinction revealed by paired sulfate–pyrite δ34S. *Earth and Planetary Science Letters*, *363*, 144–155.

Jørgensen, B. B. (1982). Mineralization of organic matter in the sea bed- the role of sulphate reduction. *Nature*, *296*, 643–645.

Kah, L. C., Lyons, T. W., & Frank, T. D. (2004). Low marine sulphate and protracted oxygenation of the Proterozoic biosphere. *Nature*, *431*, 834–838.

Kah, L. C., Thompson, C. K., Henderson, M. A., & Zhan, R. (2016). Behavior of marine sulfur in the Ordovician. *Palaeogeography, Palaeoclimatology, Palaeoecology*, *458*, 133–153. https://doi.org/10.1016/j.palaeo.2015.12.028

Kaiho, K., Kajiwara, Y., Nakano, T., Miura, Y., Kawahata, H., Tazaki, K., et al. (2001). End-Permian catastrophe by a bolide impact: Evidence of a gigantic release of sulfur from the mantle. *Geology*, *29*, 815–818. https://doi.org/10.1130/0091-7613(2001)029<0815:epcbab>2.0.co;2

Kaiho, Kunio, Kajiwara, Y., Tazaki, K., Ueshima, M., Takeda, N., Kawahata, H., et al. (1999). Oceanic primary productivity and dissolved oxygen levels at the Cretaceous/Tertiary boundary: their decrease, subsequent warming, and recovery. *Paleoceanography*, *14*(4), 511–524.

Kaiho, Kunio, Kajiwara, Y., Chen, Z.-Q., & Gorjan, P. (2006). A sulfur isotope event at the end of the Permian. *Chemical Geology*, *235*(1–2), 33–47. https://doi.org/10.1016/j.chemgeo.2006.06.001

Kampschulte, A., & Strauss, H. (2004). The sulfur isotopic evolution of Phanerozoic seawater based on the analysis of structurally substituted sulfate in carbonates. *Chemical Geology*, *204*, 255–286. https://doi.org/10.1016/j.chemgeo.2003.11.013

Kampschulte, A., Bruckschen, P., & Strauss, H. (2001). The sulphur isotopic composition of trace sulphates in Carboniferous brachiopods: implications for coeval seawater, correlation with other geochemical cycles and isotope stratigraphy. *Chemical Geology*, *175*, 149–173. https://doi.org/10.1016/s0009-2541(00)00367-3

Kampschulte, Anke. (2001). *Schwefelisotopenuntersuchungen an strukturell substituierten Sulfaten in marinen Karbonaten des Phanerozoikums : Implikationen für die geochemische Evolution des Meerwassers und die Korrelation verschiedener Stoffkreisläufe*. Ruhr-Universität Bochum. Retrieved from http://www-brs.ub.ruhr-uni-bochum.de/netahtml/HSS/Diss/KampschulteAnke/

Kaplan, I. R., Emery, K. O., & Rittenberg, S. C. (1963). The distribution and isotopic abundance of sulphur in recent marine sediments off southern California. *Geochimica et Cosmochimica Acta*, *27*(4), 297–331. https://doi.org/10.1016/0016-7037(63)90074-7

Kaufmann, B. (2006). Calibrating the Devonian Time Scale: A synthesis of U–Pb ID–TIMS ages and conodont stratigraphy. *Earth-Science Reviews*, *76*(3–4), 175–190. https://doi.org/10.1016/j.earscirev.2006.01.001

Kendall, A. C., & Harwood, G. M. (1989). Shallow-Water Gypsum in the Castile Formation - Significance and Implications. In P. M. Harris & G. A. Grover (Eds.), *Subsurface and Outcrop Examination of the Capitan Shelf Margin, Northern Delaware Basin* (pp. 451–457). San Antonio, Texas: SEPM. Retrieved from https://pubs.geoscienceworld.org/books/book/1170/chapter/10575312/shallow-water-gypsum-in-the-castile-formation

Kerans, C., & Tinker, S. W. (1999). Extrinsic stratigraphic controls on development of the Capitan Reef Complex. In A. H. Saller, P. M. Harris, B. L. Kirkland, & S. J. Mazzullo (Eds.), *Geologic Framework of the Capitan Reef*. Tulsa, Oklahoma: SEPM (Society for Sedimentary Geology).

Kolonic, S., Wagner, T., Forster, A., Sinninghe Damsté, J. S., Walsworth-Bell, B., Erba, E., et al. (2005). Black shale deposition on the northwest African Shelf during the Cenomanian/Turonian oceanic anoxic event: Climate coupling and global organic carbon burial: BLACK SHALE DEPOSITION DURING THE CENOMA. *Paleoceanography*, *20*(1), n/a-n/a. https://doi.org/10.1029/2003PA000950

Korte, C., Kozur, H., Joachimski, M., Strauss, H., Veizer, J., & Schwark, L. (2004). Carbon, sulfur, oxygen and strontium isotope records, organic geochemistry and biostratigraphy across the Permian/Triassic boundary in Abadeh, Iran. *International Journal of Earth Sciences*, *93*(4), 565–581. https://doi.org/10.1007/s00531-004-0406-7

Kozik, N. P., Young, S. A., Bowman, C. N., Saltzman, M. R., & Them, T. R. (2019). Middle–Upper Ordovician (Darriwilian–Sandbian) paired carbon and sulfur isotope stratigraphy from the Appalachian Basin, USA: Implications for dynamic redox conditions spanning the peak of the Great Ordovician Biodiversification Event. *Palaeogeography, Palaeoclimatology, Palaeoecology*, *520*, 188–202. https://doi.org/10.1016/j.palaeo.2019.01.032

Kramm, U., & Wedepohl, K. H. (1991). The isotopic composition of strontium and sulfur in seawater of Late Permian (Zechstein) age. *Chemical Geology*, *90*(3), 253–262. https://doi.org/10.1016/0009-2541(91)90103-X

Kump, L. R., & Garrels, R. M. (1986). Modeling atmospheric O 2 in the global sedimentary redox cycle. *American Journal of Science*, *286*(5), 337–360. https://doi.org/10.2475/ajs.286.5.337

Kurtz, A. C., Kump, L. R., Arthur, M. A., Zachos, J. C., & Paytan, A. (2003). Early Cenozoic decoupling of the global carbon and sulfur cycles. *Paleoceanography*, *18*(4), 1090. https://doi.org/10.1029/2003PA000908

Li, P., Huang, J., Chen, M., & Bai, X. (2009). Coincident negative shifts in sulfur and carbon isotope compositions prior to the end-Permian mass extinction at Shangsi Section of Guangyuan, South China. *Frontiers of Earth Science in China*, *3*(1), 51–56. https://doi.org/10.1007/s11707-009-0018-4

Longinelli, A., & Flora, O. (2007). Isotopic composition of gypsum samples of Permian and Triassic age from the north-eastern Italian Alps: Palaeoenvironmental implications. *Chemical Geology*, *245*(3), 275–284. https://doi.org/10.1016/j.chemgeo.2007.08.009

Loprieno, A., Bousquet, R., Bucher, S., Ceriani, S., Dalla Torre, F. H., Fügenschuh, B., & Schmid, S. M. (2011). The Valais units in Savoy (France): a key area for understanding the palaeogeography and the tectonic evolution of the Western Alps. *International Journal of Earth Sciences*, *100*(5), 963–992. https://doi.org/10.1007/s00531-010-0595-1

Lowenstein, T. K., Hardie, L. A., Timofeeff, M. N., & Demicco, R. V. (2003). Secular variation in seawater chemistry and the origin of calcium chloride basinal brines. *Geology*, *31*(10), 857–860. https://doi.org/10.1130/G19728r.1

Loyd, S. J., Marenco, P. J., Hagadorn, J. W., Lyons, T. W., Kaufman, A. J., Sour-Tovar, F., & Corsetti, F. A. (2012). Sustained low marine sulfate concentrations from the Neoproterozoic to the Cambrian: Insights from carbonates of northwestern Mexico and eastern California. *Earth and Planetary Science Letters*, *339–340*(0), 79–94. https://doi.org/10.1016/j.epsl.2012.05.032

Lu, F. H., & Meyers, W. J. (2003). Sr, S, and OSO4 Isotopes and the Depositional Environments of the Upper Miocene Evaporites, Spain. *Journal of Sedimentary Research*, *73*(3), 444–450. https://doi.org/10.1306/093002730444

Luo, G., Kump, L. R., Wang, Y., Tong, J., Arthur, M. A., Yang, H., et al. (2010). Isotopic evidence for an anomalously low oceanic sulfate concentration following end-Permian mass extinction. *Earth and Planetary Science Letters*, *300*(1–2), 101–111. https://doi.org/10.1016/j.epsl.2010.09.041

Lyons, T. W., Walter, L. M., Gellatly, A. M., Martini, A. M., & Blake, R. E. (2004). Sites of anomalous organic remineralization in the carbonate sediments of South Florida, USA: The sulfur cycle and carbonate-associated sulfate. In J. P. Amend, K. J. Edwards, & T. W. Lyons (Eds.), *Sulfur Biogeochemistry - Past and Present* (pp. 161–176). Boulder, Colorado: Geological Society of America.

Lyu, Z., Zhang, L., Algeo, T. J., Zhao, L., Chen, Z.-Q., Li, C., et al. (2019). Global-ocean circulation changes during the Smithian–Spathian transition inferred from carbon-sulfur cycle records. *Earth-Science Reviews*. https://doi.org/10.1016/j.earscirev.2019.01.010

Maharjan, D., Jiang, G., Peng, Y., & Nicholl, M. J. (2018). Sulfur isotope change across the Early Mississippian K–O (Kinderhookian–Osagean) δ 13 C excursion. *Earth and Planetary Science Letters*, *494*, 202–215. https://doi.org/10.1016/j.epsl.2018.04.043

Marenco, P. J., Corsetti, F. A., Kaufman, A. J., & Bottjer, D. J. (2008). Environmental and diagenetic variations in carbonate associated sulfate: An investigation of CAS in the Lower Triassic of the western USA. *Geochimica et Cosmochimica Acta*, *72*, 1570–1582.

Marenco, Pedro J., Marenco, K. N., Lubitz, R. L., & Niu, D. (2013). Contrasting long-term global and short-term local redox proxies during the Great Ordovician Biodiversification Event: A case study from Fossil Mountain, Utah, USA. *Palaeogeography, Palaeoclimatology, Palaeoecology*, *377*, 45–51. https://doi.org/10.1016/j.palaeo.2013.03.007

Marenco, Pedro J., Martin, K. R., Marenco, K. N., & Barber, D. C. (2016). Increasing global ocean oxygenation and the Ordovician Radiation: Insights from Th/U of carbonates from the Ordovician of western Utah. *Palaeogeography, Palaeoclimatology, Palaeoecology*, *458*, 77–84. https://doi.org/10.1016/j.palaeo.2016.05.014

Martin, E. E., & Scher, H. D. (2004). Preservation of seawater Sr and Nd isotopes in fossil fish teeth: bad news and good news. *Earth and Planetary Science Letters*, *220*(1), 25–39. https://doi.org/10.1016/S0012-821X(04)00030-5

Mazzullo, S. J. (1982). Stratigraphy and Depositional Mosaics of Lower Clear Fork and Wichita Groups (Permian), Northern Midland Basin, Texas. *AAPG Bulletin*, *66*(2), 210–227. https://doi.org/10.1306/03B59A67-16D1-11D7-8645000102C1865D

Mekhtiyeva, V. (1974). Sulfur isotopic composition of fossil molluscan shells as an indicator of hydrochemical conditions in ancient basins. *Geochemistry International*, *11*, 1188–1192.

Meng, F.-W., Zhang, Z., Yan, X., Ni, P., Liu, W.-H., Fan, F., & Xie, G.-W. (2019). Stromatolites in Middle Ordovician carbonate–evaporite sequences and their carbon and sulfur isotopes stratigraphy, Ordos Basin, northwestern China. *Carbonates and Evaporites*, *34*(1), 11–20. https://doi.org/10.1007/s13146-017-0367-0

Meng, F.-W., Zhang, Z., Schiffbauer, J. D., Zhuo, Q., Zhao, M., Ni, P., et al. (2019). The Yudomski event and subsequent decline: new evidence from δ34S data of lower and middle Cambrian evaporites in the Tarim Basin, western China. *Carbonates and Evaporites*, *34*(3), 1117–1129. https://doi.org/10.1007/s13146-017-0407-9

Meyers Stephen R., Sageman Bradley B., & Arthur Michael A. (2012). Obliquity forcing of organic matter accumulation during Oceanic Anoxic Event 2. *Paleoceanography*, *27*(3). https://doi.org/10.1029/2012PA002286

Mills, J. V., Gomes, M. L., Kristall, B., Sageman, B. B., Jacobson, A. D., & Hurtgen, M. T. (2017). Massive volcanism, evaporite deposition, and the chemical evolution of the Early Cretaceous ocean. *Geology*, *45*(5), 475–478. https://doi.org/10.1130/G38667.1

Newton, R. J., Pevitt, E. L., Wignall, P. B., & Bottrell, S. H. (2004). Large shifts in the isotopic composition of seawater sulphate across the Permo–Triassic boundary in northern Italy. *Earth and Planetary Science Letters*, *218*, 331–345. https://doi.org/10.1016/S0012-821X(03)00676-9

Newton, R. J., Reeves, E. P., Kafousia, N., Wignall, P. B., Bottrell, S. H., & Sha, J. (2011). Low marine sulfate concentrations and the isolation of the European epicontinental sea during the Early Jurassic. *Geology*, *39*, 7–10. https://doi.org/10.1130/g31326.1

Nielsen, H. (1989). Local and global aspects of the sulphur isotope age curve of oceanic sulphate. *Evolution of the Global Biogeochemical Sulphur Cycle. Wiley, New York*, 57–64.

Nielsen, H., & Ricke, W. (1964). Schwefel-isotopen verhältnisse von evaporiten aus deutschland; Ein beitrag zur kenntnis von δ34S im meerwasser-sulfat. *Geochimica et Cosmochimica Acta*, *28*(5), 577–591. https://doi.org/10.1016/0016-7037(64)90078-X

Novikov, D. A. (2017). Distribution of Cambrian salts in the western Siberian craton (Yurubcheno-Tokhomo field, Russia). *Arabian Journal of Geosciences*, *10*(1). https://doi.org/10.1007/s12517-016-2792-0

Ohkouchi, N., Kawamura, K., Kajiwara, Y., Wada, E., Okada, M., Kanamatsu, T., & Taira, A. (1999). Sulfur isotope records around Livello Bonarelli (northern Apennines, Italy) black shale at the Cenomanian-Turonian boundary. *Geology*, *27*, 535–538. https://doi.org/10.1130/0091-7613(1999)027<0535:siralb>2.3.co;2

Owens, J. D., Gill, B. C., Jenkyns, H. C., Bates, S. M., Severmann, S., Kuypers, M. M. M., et al. (2013). Sulfur isotopes track the global extent and dynamics of euxinia during Cretaceous Oceanic Anoxic Event 2. *Proceedings of the National Academy of Sciences*, *110*(46), 18407–18412. https://doi.org/10.1073/pnas.1305304110

Pankina, R. G., Maksimov, S. P., Kalinko, M. K., Monakhov, I. B., & Guriyeva, S. M. (1975). Sulfur isotopic composition in the Phanerozoic evaporites of Bulgaria. *Geochemistry International*, *12*(6), 79–83.

Paris, G., Sessions, A. L., Subhas, A. V., & Adkins, J. F. (2013). MC-ICP-MS measurement of δ34S and Δ33S in small amounts of dissolved sulfate. *Chemical Geology*, *345*, 50–61. https://doi.org/10.1016/j.chemgeo.2013.02.022

Paris, G., Fehrenbacher, J. S., Sessions, A. L., Spero, H. J., & Adkins, J. F. (2014). Experimental determination of carbonate-associated sulfate δ34S in planktonic foraminifera shells. *Geochemistry, Geophysics, Geosystems*, *15*(4), 1452–1461. https://doi.org/10.1002/2014GC005295

Paris, G., Adkins, J. F., Sessions, A. L., Webb, S. M., & Fischer, W. W. (2014). Neoarchean carbonate–associated sulfate records positive Δ33S anomalies. *Science*, *346*(6210), 739–741. https://doi.org/10.1126/science.1258211

Paytan, A., Kastner, M., Martin, E. E., Macdougall, J. D., & Herbert, T. (1993). Marine barite as a monitor of seawater strontium isotope composition. *Nature*, *366*, 445–449.

Paytan, A., Kastner, M., Campbell, D., & Thiemens, M. H. (1998). Sulfur Isotopic Composition of Cenozoic Seawater Sulfate. *Science*, *282*, 1459–1462. https://doi.org/10.1126/science.282.5393.1459

Paytan, A., Mearon, S., Cobb, K., & Kastner, M. (2002). Origin of marine barite deposits: Sr and S isotope characterization. *Geology*, *30*, 747–750. https://doi.org/10.1130/0091-7613(2002)030<0747:oombds>2.0.co;2

Paytan, A., Kastner, M., Campbell, D., & Thiemens, M. H. (2004). Seawater Sulfur Isotope Fluctuations in the Cretaceous. *Science*, *304*, 1663–1665. https://doi.org/10.1126/science.1095258

Peryt, T. M., Halas, S., & Hryniv, S. P. (2010). Sulphur and oxygen isotope signatures of late Permian Zechstein anhydrites, West Poland: seawater evolution and diagenetic constraints. *Geological Quarterly*, *54*, 387–400.

Pisarchik, Y. K., & Golubchina, M. N. (1975). On isotope ratios of sulfur in the Cambrian sulfatic limestones of the Siberian platform. *Geochemistry International*, *12*, 227–230.

Playà, E., Cendón, D. I., Travé, A., Chivas, A. R., & García, A. (2007). Non-marine evaporites with both inherited marine and continental signatures: The Gulf of Carpentaria, Australia, at ~70 ka. *Sedimentary Geology*, *201*(3–4), 267–285. https://doi.org/10.1016/j.sedgeo.2007.05.010

Pope, M. C., & Grotzinger, J. P. (2003). Paleoproterozoic Stark Formation, Athapuscow Basin, Northwest Canada: Record of Cratonic-Scale Salinity Crisis. *Journal of Sedimentary Research*, *73*(2), 280–295. https://doi.org/10.1306/091302730280

Posey, H. H., & Fisher, S. R. (1989). A sulfur and strontium isotopic investigation of Lower Permian anhydrite, Palo Duro Basin, Texas, U.S.A. *Applied Geochemistry*, *4*(4), 395–407. https://doi.org/10.1016/0883-2927(89)90015-2

Poulton, S. W., Henkel, S., März, C., Urquhart, H., Flögel, S., Kasten, S., et al. (2015). A continental-weathering control on orbitally driven redox-nutrient cycling during Cretaceous Oceanic Anoxic Event 2. *Geology*, *43*(11), 963–966. https://doi.org/10.1130/G36837.1

Present, T. M. (2018). *Controls on the Sulfur Isotopic Composition of Carbonate-Associated Sulfate* (Ph.D.). California Institute of Technology, Pasadena, California. Retrieved from http://resolver.caltech.edu/CaltechTHESIS:04042018-153105432

Present, T. M., Paris, G., Burke, A., Fischer, W. W., & Adkins, J. F. (2015). Large Carbonate Associated Sulfate isotopic variability between brachiopods, micrite, and other sedimentary components in Late Ordovician strata. *Earth and Planetary Science Letters*, *432*, 187–198. https://doi.org/10.1016/j.epsl.2015.10.005

Present, T. M., Gutierrez, M., Paris, G., Kerans, C., Grotzinger, J. P., & Adkins, J. F. (2019). Diagenetic controls on the isotopic composition of carbonate-associated sulphate in the Permian Capitan Reef Complex, West Texas. *Sedimentology*, *66*(7), 2605–2626. https://doi.org/10.1111/sed.12615

Prokoph, A., Shields, G. A., & Veizer, J. (2008). Compilation and time-series analysis of a marine carbonate δ18O, δ13C, 87Sr/86Sr and δ34S database through Earth history. *Earth-Science Reviews*, *87*(3–4), 113–133. https://doi.org/10.1016/j.earscirev.2007.12.003

Qiu, Z., Sun, S., Wei, H., Wang, Q., Zou, C., & Zhang, Y. (2015). SIMS zircon U-Pb dating from bentonites in the Penglaitan Global Stratotype Section for the Guadalupian–Lopingian boundary (GLB), South China. *Geological Journal*.

Raab, M., & Spiro, B. (1991). Sulfur isotopic variations during seawater evaporation with fractional crystallization. *Chemical Geology: Isotope Geoscience Section*, *86*(4), 323–333. https://doi.org/10.1016/0168-9622(91)90014-N

Rennie, V. C. F., & Turchyn, A. V. (2014). The preservation of d34SSO4 and d18OSO4 in carbonate-associated sulfate during marine diagenesis: A 25 Myr test case using marine sediments. *Earth and Planetary Science Letters*, *395*, 13–23. https://doi.org/10.1016/j.epsl.2014.03.025

Rennie, V. C. F., Paris, G., Sessions, A. L., Abramovich, S., Turchyn, A. V., & Adkins, J. F. (2018). Cenozoic record of δ 34 S in foraminiferal calcite implies an early Eocene

shift to deep-ocean sulfide burial. *Nature Geoscience*, (11), 761–765. https://doi.org/10.1038/s41561-018-0200-y

Riccardi, A. L., Arthur, M. A., & Kump, L. R. (2006). Sulfur isotopic evidence for chemocline upward excursions during the end-Permian mass extinction. *Geochimica et Cosmochimica Acta*, *70*, 5740–5752.

Richardson, J. A., Keating, C., Lepland, A., Hints, O., Bradley, A. S., & Fike, D. A. (2019). Silurian records of carbon and sulfur cycling from Estonia: The importance of depositional environment on isotopic trends. *Earth and Planetary Science Letters*, *512*, 71–82. https://doi.org/10.1016/j.epsl.2019.01.055

Rine, M. J., Garrett, J. D., & Kaczmarek, S. E. (2017). A New Facies Architecture Model for the Silurian Niagaran Pinnacle Reef Complexes of the Michigan Basin. In A. J. Macneil, J. Lonnee, & R. Wood, *Characterization and Modeling of Carbonates–Mountjoy Symposium 1*. SEPM (Society for Sedimentary Geology). https://doi.org/10.2110/sepmsp.109.02

Rose, C. V., Fischer, W. W., Finnegan, S., & Fike, D. A. (2019). Records of carbon and sulfur cycling during the Silurian Ireviken Event in Gotland, Sweden. *Geochimica et Cosmochimica Acta*, *246*, 299–316. https://doi.org/10.1016/j.gca.2018.11.030

Sakai, H. (1972). Oxygen isotopic ratios of some evaporites from Precambrian to Recent ages. *Earth and Planetary Science Letters*, *15*(2), 201–205. https://doi.org/10.1016/0012-821X(72)90061-1

Saltzman, M. R., Cowan, C. A., Runkel, A. C., Runnegar, B., Stewart, M. C., & Palmer, A. R. (2004). The Late Cambrian Spice (δ13C) Event and the Sauk II-SAUK III Regression: New Evidence from Laurentian Basins in Utah, Iowa, and Newfoundland. *Journal of Sedimentary Research*, *74*(3), 366–377. https://doi.org/10.1306/120203740366

Schobben, M., Stebbins, A., Ghaderi, A., Strauss, H., Korn, D., & Korte, C. (2015). Flourishing ocean drives the end-Permian marine mass extinction. *Proceedings of the National Academy of Sciences*, *112*(33), 10298–10303. https://doi.org/10.1073/pnas.1503755112

Schobben, M., Stebbins, A., Algeo, T. J., Strauss, H., Leda, L., Haas, J., et al. (2017). Volatile earliest Triassic sulfur cycle: A consequence of persistent low seawater sulfate concentrations and a high sulfur cycle turnover rate? *Palaeogeography, Palaeoclimatology, Palaeoecology*, *486*, 74–85. https://doi.org/10.1016/j.palaeo.2017.02.025

Schrag, D. P., DePaolo, D. J., & Richter, F. M. (1995). Reconstructing past sea surface temperatures: Correcting for diagenesis of bulk marine carbonate. *Geochimica et Cosmochimica Acta*, *59*(11), 2265–2278. https://doi.org/10.1016/0016-7037(95)00105-9

Schröder, S., Schreiber, B. C., Amthor, J. E., & Matter, A. (2004). Stratigraphy and environmental conditions of the terminal Neoproterozoic–Cambrian Period in Oman: evidence from sulphur isotopes. *Journal of the Geological Society*, *161*(3), 489–499. https://doi.org/10.1144/0016-764902-062

Sim, M. S., Ono, S., & Hurtgen, M. T. (2015). Sulfur isotope evidence for low and fluctuating sulfate levels in the Late Devonian ocean and the potential link with the

mass extinction event. *Earth and Planetary Science Letters*, *419*, 52–62. https://doi.org/10.1016/j.epsl.2015.03.009

Solomon, M., Rafter, T. A., & Dunham, K. C. (1971). Sulphur and oxygen isotope studies in the northern Pennines in relation to ore genesis. *Transactions of the Institution of Mining and Metallurgy Section B*, *80B*, 259–275.

Song, H., Tong, J., Algeo, T. J., Song, H., Qiu, H., Zhu, Y., et al. (2014). Early Triassic seawater sulfate drawdown. *Geochimica et Cosmochimica Acta*, *128*(0), 95–113. https://doi.org/10.1016/j.gca.2013.12.009

Song, H., Du, Y., Algeo, T. J., Tong, J., Owens, J. D., Song, H., et al. (2019). Cooling-driven oceanic anoxia across the Smithian/Spathian boundary (mid-Early Triassic). *Earth-Science Reviews*. https://doi.org/10.1016/j.earscirev.2019.01.009

Spötl, C. (1988). Schwefelisotopendatierungen und fazielle Entwicklung permoskytischer Anhydrite in den Salzbergbauen von Dürrnberg/Hallstein und Hallstadt (Österreich). *Mitteilungen Der Gesellschaft Der Geologie- Und Bergbaustudenten in Österreich*, *34–35*, 209–229.

Staudt, W. J., & Schoonen, M. A. A. (1995). Sulfate Incorporation into Sedimentary Carbonates. In *Geochemical Transformations of Sedimentary Sulfur* (Vol. 612, pp. 332–345). American Chemical Society. https://doi.org/10.1021/bk-1995-0612.ch018

Stebbins, A., Algeo, T. J., Krystyn, L., Rowe, H., Brookfield, M., Williams, J., et al. (2019). Marine sulfur cycle evidence for upwelling and eutrophic stresses during Early Triassic cooling events. *Earth-Science Reviews*. https://doi.org/10.1016/j.earscirev.2018.09.007

Stollhofen, H., Bachmann, G. H., Barnasch, J., Bayer, U., Beutler, G., Franz, M., et al. (2008). Upper Rotliegend to early cretaceous basin development. *Dynamics of Complex Intracontinental Basins. The Central European Basin System*, 181–210.

Strauss, H. (1997). The isotopic composition of sedimentary sulfur through time. *Palaeogeography, Palaeoclimatology, Palaeoecology*, *132*, 97–118. https://doi.org/10.1016/s0031-0182(97)00067-9

Taki, H. E., & Pratt, B. R. (2012). Syndepositional tectonic activity in an epicontinental basin revealed by deformation of subaqueous carbonate laminites and evaporites: Seismites in Red River strata (Upper Ordovician) of southern Saskatchewan, Canada. *Bulletin of Canadian Petroleum Geology*, *60*(1), 37–58. https://doi.org/10.2113/gscpgbull.60.1.37

Thode, H. G., & Monster, J. (1965). Sulfur-Isotope Geochemistry of Petroleum, Evaporites, and Ancient Seas. In A. Young & J. E. Galley (Eds.), *AAPG Memoir 4: Fluids in subsurface environments* (Vol. 71, pp. 367–377). Tulsa, Oklahoma: American Association of Petroleum Geologists. Retrieved from http://archives.datapages.com/data/specpubs/methodo2/data/a071/a071/0001/0350/0367.htm

Thode, H. G., & Monster, J. (1970). Sulfur Isotope Abundances and Genetic Relations of Oil Accumulations in Middle East Basin. *AAPG Bulletin*, *54*(4), 627–637.

Thode, H. G., Macnamara, J., & Fleming, W. H. (1953). Sulphur isotope fractionation in nature and geological and biological time scales. *Geochimica et Cosmochimica Acta*, *3*(5), 235–243. https://doi.org/10.1016/0016-7037(53)90042-8

Thode, H. G., Monster, J., & Dunford, H. B. (1958). Sulphur Isotope Abundances in Petroleum and Associated Materials. *AAPG Bulletin*, *42*(11), 2619–2641.

Thompson, Cara K., & Kah, L. C. (2012). Sulfur isotope evidence for widespread euxinia and a fluctuating oxycline in Early to Middle Ordovician greenhouse oceans. *Palaeogeography, Palaeoclimatology, Palaeoecology*, *313–314*(0), 189–214. https://doi.org/10.1016/j.palaeo.2011.10.020

Thompson, Cara K., Kah, L. C., Astini, R., Bowring, S. A., & Buchwaldt, R. (2012). Bentonite geochronology, marine geochemistry, and the Great Ordovician Biodiversification Event (GOBE). *Palaeogeography, Palaeoclimatology, Palaeoecology*, *321–322*(0), 88–101. https://doi.org/10.1016/j.palaeo.2012.01.022

Thompson, Cara Kim. (2011). *Carbon and Sulfur Cycling in Early Paleozoic Oceans* (Ph.D. diss). University of Tennessee, Knoxville.

Toggweiler, J. R., & Sarmiento, J. L. (1985). Glacial to Interglacial Changes in Atmospheric Carbon Dioxide: The Critical Role of Ocean Surface Water in High Latitudes. In *The Carbon Cycle and Atmospheric CO2: Natural Variations Archean to Present* (pp. 163–184). American Geophysical Union (AGU). https://doi.org/10.1029/GM032p0163

Torres, M. A., West, A. J., & Li, G. (2014). Sulphide oxidation and carbonate dissolution as a source of CO_2 over geological timescales. *Nature*, *507*(7492), 346–349. https://doi.org/10.1038/nature13030

Torres, M. E., Brumsack, H. J., Bohrmann, G., & Emeis, K. C. (1996). Barite fronts in continental margin sediments: a new look at barium remobilization in the zone of sulfate reduction and formation of heavy barites in diagenetic fronts. *Chemical Geology*, *127*, 125–139. https://doi.org/10.1016/0009-2541(95)00090-9

Turchyn, A. V., Schrag, D. P., Coccioni, R., & Montanari, A. (2009). Stable isotope analysis of the Cretaceous sulfur cycle. *Earth and Planetary Science Letters*, *285*, 115–123. https://doi.org/10.1016/j.epsl.2009.06.002

Turchyn, Alexandra V., & DePaolo, D. J. (2019). Seawater Chemistry Through Phanerozoic Time. *Annual Review of Earth and Planetary Sciences*, *47*(1), 197–224. https://doi.org/10.1146/annurev-earth-082517-010305

Utrilla, R., Pierre, C., Orti, F., & Pueyo, J. J. (1992). Oxygen and sulphur isotope compositions as indicators of the origin of Mesozoic and Cenozoic evaporites from Spain. *Chemical Geology*, *102*(1), 229–244. https://doi.org/10.1016/0009-2541(92)90158-2

Veizer, J., Holser, W. T., & Wilgus, C. K. (1980). Correlation of 13C12C and 34S32S secular variations. *Geochimica et Cosmochimica Acta*, *44*(4), 579–587. https://doi.org/10.1016/0016-7037(80)90250-1

Vinogradov, V. I. (2007). Was there a conflict at the Neoproterozoic-Cambrian boundary: Evidence from sulfur isotope composition? *Lithology and Mineral Resources*, *42*(1), 1–14. https://doi.org/10.1134/S0024490207010014

Voigt, S., Erbacher, J., Mutterlose, J., Weiss, W., Westerhold, T., Wiese, F., et al. (2008). The Cenomanian – Turonian of the Wunstorf section – (North Germany): global stratigraphic reference section and new orbital time scale for Oceanic Anoxic Event 2.

Newsletters on Stratigraphy, *43*(1), 65–89. https://doi.org/10.1127/0078-0421/2008/0043-0065

Vredenburgh, L. D., & Cheney, E. S. (1971). Sulfur and carbon isotopic investigation of petroleum, Wind River basin, Wyoming. *AAPG Bulletin*, *55*(11), 1954–1975.

Walker, J. C. (1986). Global geochemical cycles of carbon, sulfur and oxygen. *Marine Geology*, *70*(1), 159–174.

Warren, J. K. (2010). Evaporites through time: Tectonic, climatic and eustatic controls in marine and nonmarine deposits. *Earth-Science Reviews*, *98*(3), 217–268. https://doi.org/10.1016/j.earscirev.2009.11.004

Webster, R., & Oliver, M. A. (2007). *Geostatistics for environmental scientists* (2nd ed.). Chichester, UK: Wiley.

Wei, W., & Gartner, S. (1993). 2. Neogene Calcareous Nannofossils from Sites 811 and 819 Through 825, offshore Northeastern Australia. In J. A. McKenzie, P. J. Davies, & A. Palmer-Julson (Eds.), *Scientific Results* (Vol. 133, pp. 19–37). College Station, Texas: Ocean Drilling Program. https://doi.org/10.2973/odp.proc.sr.133.1993

Westerhold, T., Röhl, U., Raffi, I., Fornaciari, E., Monechi, S., Reale, V., et al. (2008). Astronomical calibration of the Paleocene time. *Palaeogeography, Palaeoclimatology, Palaeoecology*, *257*(4), 377–403. https://doi.org/10.1016/j.palaeo.2007.09.016

Witts, J. D., Newton, R. J., Mills, B. J. W., Wignall, P. B., Bottrell, S. H., Hall, J. L. O., et al. (2018). The impact of the Cretaceous–Paleogene (K–Pg) mass extinction event on the global sulfur cycle: Evidence from Seymour Island, Antarctica. *Geochimica et Cosmochimica Acta*. https://doi.org/10.1016/j.gca.2018.02.037

Worden, R. H., Smalley, P. C., & Fallick, A. E. (1997). Sulfur cycle in buried evaporites. *Geology*, *25*(7), 643–646. https://doi.org/10.1130/0091-7613(1997)025<0643:SCIBE>2.3.CO;2

Wotte, T., Strauss, H., & Sundberg, F. A. (2011). Carbon and Sulfur Isotopes from the Cambrian Series 2-Cambrian Series 3 of Laurentia and Siberia. In J. S. Hollingsworth, F. A. Sundberg, & J. R. Foster (Eds.), *Museum of Northern Arizona Bulletin 67: Cambrian Stratigraphy and Paleontology of Northern Arizona and Southern Nevada: The 16th Field Conference of the Cambrian Stage Subdivision Working Group, International Subcommission on Cambrian Stratigraphy, Flagstaff, Arizona, and Southern Nevada, United States* (pp. 43–63). Flagstaff, Arizona: Museum of Northern Arizona.

Wotte, T., Shields-Zhou, G. A., & Strauss, H. (2012). Carbonate-associated sulfate: Experimental comparisons of common extraction methods and recommendations toward a standard analytical protocol. *Chemical Geology*, *326–327*, 132–144. https://doi.org/10.1016/j.chemgeo.2012.07.020

Wright, J. D., & Kroon, D. (2000). Planktonic foraminiferal biostratigraphy of Leg 166. In P. K. Swart, G. P. Eberli, M. J. Malone, & J. F. Sarg (Eds.), *Scientific Results* (Vol. 166, pp. 3–12). College Station, Texas: Ocean Drilling Program. https://doi.org/10.2973/odp.proc.sr.166.2000

Wu, N. (2013). *Sulfur isotopic evolution of Phanerozoic and Ediacaran seawater sulfate*. University of Maryland, College Park, Md. Retrieved from http://hdl.handle.net/1903/14016

Wu, N., Farquhar, J., & Strauss, H. (2014). δ34S and Δ33S records of Paleozoic seawater sulfate based on the analysis of carbonate associated sulfate. *Earth and Planetary Science Letters*, *399*(0), 44–51. https://doi.org/10.1016/j.epsl.2014.05.004

Wu, Q., Ramezani, J., Zhang, H., Yuan, D., Erwin, D. H., Henderson, C. M., et al. (2020). High-precision U-Pb zircon age constraints on the Guadalupian in West Texas, USA. *Palaeogeography, Palaeoclimatology, Palaeoecology*, *548*, 109668. https://doi.org/10.1016/j.palaeo.2020.109668

Yadong, S., Xulong, L., Haishui, J., Genming, L., Si, S., Chunbo, Y., & Wignall, P. B. (2008). Guadalupian (Middle Permian) Conodont Faunas at Shangsi Section, Northeast Sichuan Province. *Journal of China University of Geosciences*, *19*(5), 451–460. https://doi.org/10.1016/S1002-0705(08)60050-3

Yan, D., Zhang, L., & Qiu, Z. (2013). Carbon and sulfur isotopic fluctuations associated with the end-Guadalupian mass extinction in South China. *Gondwana Research*, *24*(3–4), 1276–1282. https://doi.org/10.1016/j.gr.2013.02.008

Yang, C., Li, X.-H., Zhu, M., Condon, D. J., & Chen, J. (2018). Geochronological constraint on the Cambrian Chengjiang biota, South China. *Journal of the Geological Society*, *175*(4), 659–666. https://doi.org/10.1144/jgs2017-103

Yao, W., Paytan, A., & Wortmann, U. G. (2018). Large-scale ocean deoxygenation during the Paleocene-Eocene Thermal Maximum. *Science*, *361*(6404), 804–806. https://doi.org/10.1126/science.aar8658

Yao, W., Paytan, A., Griffith, E. M., Martínez-Ruiz, F., Markovic, S., & Wortmann, U. G. (2020). A revised seawater sulfate S-isotope curve for the Eocene. *Chemical Geology*, *532*, 119382. https://doi.org/10.1016/j.chemgeo.2019.119382

Yeremenko, N. A., & Pankina, R. G. (1972). Variations of 34S in Sulfates of Recent and Ancient Marine Basins of the Soviet Union. *Geochemistry International*, *10*, 45–54.

Young, S. A., Gill, B. C., Edwards, C. T., Saltzman, M. R., & Leslie, S. A. (2016). Middle–Late Ordovician (Darriwilian–Sandbian) decoupling of global sulfur and carbon cycles: Isotopic evidence from eastern and southern Laurentia. *Palaeogeography, Palaeoclimatology, Palaeoecology*, *458*, 118–132. https://doi.org/10.1016/j.palaeo.2015.09.040

Young, S. A., Kleinberg, A., & Owens, J. D. (2019). Geochemical evidence for expansion of marine euxinia during an early Silurian (Llandovery–Wenlock boundary) mass extinction. *Earth and Planetary Science Letters*, *513*, 187–196. https://doi.org/10.1016/j.epsl.2019.02.023

Zhang, L., Zhao, L., Chen, Z.-Q., Algeo, T. J., Li, Y., & Cao, L. (2015). Amelioration of marine environments at the Smithian–Spathian boundary, Early Triassic. *Biogeosciences*, *12*(5), 1597–1613.

Zhu, M., Yang, A., Yuan, J., Li, G., Zhang, J., Zhao, F., et al. (2019). Cambrian integrative stratigraphy and timescale of China. *Science China Earth Sciences*, *62*(1), 25–60. https://doi.org/10.1007/s11430-017-9291-0